EFORT open reviews

The contribution of the histopathological examination to the diagnosis of adverse local tissue reactions in arthroplasty

Giorgio Perino[1]
Ivan De Martino[2]
Lingxin Zhang[3]
Zhidao Xia[4]
Jiri Gallo[5]
Shonali Natu[6]
David Langton[7]
Monika Huber[8]
Anastasia Rakow[1]
Janosch Schoon[1]
Enrique Gomez-Barrena[9]
Veit Krenn[10]

■ The histopathological examination of the periprosthetic soft tissue and bone has contributed to the identification and description of the morphological features of adverse local tissue reactions (ALTR)/adverse reactions to metallic debris (ARMD). The need of a uniform vocabulary for all disciplines involved in the diagnosis and management of ALTR/ARMD and of clarification of the parameters used in the semi-quantitative scoring systems for their classification has been considered a pre-requisite for a meaningful interdisciplinary evaluation.

■ This review of key terms used for ALTR/ARMD has resulted in the following outcomes: (a) pseudotumor is a descriptive term for ALTR/ARMD, classifiable in two main types according to its cellular composition defining its clinical course; (b) the substitution of the term metallosis with presence of metallic wear debris, since it cannot be used as a category of implant failure or histological diagnosis; (c) the term aseptic lymphocytic-dominated vasculitis-associated lesion (ALVAL) should be replaced due to the absence of a vasculitis with ALLTR/ALRMD for lymphocytic-predominant and AMLTR/AMRMD for macrophage-predominant reaction.

■ This review of the histopathological classifications of ALTR/ARMD has resulted in the following outcomes: (a) distinction between cell death and tissue necrosis; (b) the association of corrosion metallic debris with adverse local lymphocytic reaction and tissue necrosis; (c) the importance of cell and particle debris for the viscosity and density of the lubricating synovial fluid; (d) a consensus classification of lymphocytic infiltrate in soft tissue and bone marrow; (e) evaluation of the macrophage infiltrate in soft tissues and bone marrow; (f) classification of macrophage induced osteolysis/aseptic loosening as a delayed type of ALTR/ARMD; (g) macrophage motility and migration as possible driving factor for osteolysis; (h) usefulness of the histopathological examination for the natural history of the adverse reactions, radiological correlation, post-marketing surveillance, and implant registries.

■ The review of key terms used for the description and histopathological classification of ALTR/ARMD has resulted in a comprehensive, new standard for all disciplines involved in their diagnosis, clinical management, and long-term clinical follow-up.

Background

Orthopaedic implants have been invented and used on millions of patients to restore mobility primarily for hip and knee joint replacement with remarkable changes of the materials used since their inception in the late 19th century.[1–4] The evolution of implants with the use of different materials has led to the design of prosthetic devices for other joints, such as shoulder, elbow, wrist, ankle, and small joints of the hands and feet.[5–9] Surgical pathologists, mainly through the use of the histopathological examination of the periprosthetic soft tissue and bone, have been instrumental to wear particle identification, description and semi-quantitative classification[10–13] and to the description and classification of cellular responses to implant wear debris for several decades.[14–16] Histopathological examination has also significantly contributed to the interdisciplinary assessment of mechanisms of orthopaedic implant fixation and failure with host response in the periprosthetic tissues.[17–19]

More recently, histological examination has contributed to the identification and description of the morphological features of an immunologically mediated reaction defined as aseptic failure due to a lymphocytic-dominated vasculitis associated lesion (ALVAL),[20] later expanded to adverse local tissue reactions (ALTR)[21] and adverse reactions to metal debris (ARMD)[22] associated with metal-on-metal (MoM) hip resurfacing arthroplasty (HRA) and MoM small head (SH) and large head (LH) total hip arthroplasty (THA) with/without metallic adapter sleeve (MAS) and non-MoM THA implants with metal-on-polyethylene (MoP), ceramic-on-polyethylene (CoP), and ceramic-on-ceramic (CoC) bearing surface with various head/neck junctions and CoCr dual modular neck (DMN), in two types coupled with a TMZF (Ti, Mo, Zr, Fe) stem.[20,23–29] This body of work for hip implants can also be applied to all other joint replacements with metallic junctions.

The histopathological examination has been, for decades, the only tool available, through conventional light microscopy and later also by the use of transmission and/or scanning electron microscopy (TEM/SEM), for the description of the types of cells involved in the host reaction and their relationship to the particulate materials.[30] More recently, the development of immunohistochemistry, immunofluorescence, and molecular techniques has contributed to a more refined understanding of the adverse tissue reactions and of the underlying mechanisms of cellular response.[31–35] The collection of appropriate fresh tissue and synovial fluid at surgery followed by standard histopathological examination of paraffin-embedded tissue are still fundamental for the successful performance of any subsequent in-depth analysis.[36]

Surgical pathologists have also been responsible for a large part of the terminology used to describe the ALTR/ARMD. Some terms have been incorrectly used, which has led to confusion in the scientific literature with uncertainties regarding their clinical and biological significance for diagnostic classification, clinical follow-up, and surveillance. The need for the development of a uniform vocabulary for all disciplines involved in the diagnosis and management of ALTR/ARMD and of clarification of the parameters used in the proposed semi-quantitative scoring systems for its classification has been recently emphasized.[37]

The aims of this review article on the histopathology of ALTR/ARMD are: (a) fill the current gap regarding a consistent terminology through the analysis of key pathological and clinical terms commonly used in the description of ALTR/ARMD; (b) summarize and critically analyse the current parameters which have been used for the histological classifications of ALTR/ARMD and the implications for clinical practice and surveillance; (c) enable a comprehensive evaluation of the terminology and classification used for the histopathological examination and its limitation in the assessment of the medium- and long-term local and systemic effects of the ALTR/ARMD; (d) propose a consensus terminology as a tool for minimizing contradictory results regarding the post-marketing analyses of orthopaedic implants by clinicians, regional and national implant registries, regulatory authorities, and manufacturing industry.

Methods

The cases described in this study were selected by two orthopaedic pathologists with extensive experience and scholar publications on periprosthetic tissue examination (GP, VK) with consensus agreement on the histological diagnosis. All pictures were taken with the use of a microscope camera (Zeiss Axioskop 40, Jenoptik ProgRes, Jena, Germany). The system was calibrated using a standard micrometre glass slide with 1 mm horizontal scale, 100 divisions –10μm intervals. All measures shown in the figures were taken using a calibrated eyepiece 5 mm, 100 divisions reticle.

ALTR/ARMD terminology

It is important to emphasize that both the acronyms ALTR and ARMD represent an umbrella term which is used clinically for a cohort of symptoms and radiological findings usually obtained by ultrasound, magnetic resonance imaging scans (MRI), and computerized axial tomography scans (CT) leading to the preoperative diagnosis of suspected adverse reaction to particulate wear debris. The terms ALTR/ARMD can also be used in the histopathological diagnosis, although they do not represent a specific diagnosis and need to be associated with the description of the types of inflammatory cells present in the reaction.

In this review, the terms ALTR and ARMD are used as equivalent for the cases of MoM HRA and THA implants which, by definition, can produce only metallic wear debris, and also for non-MoM prostheses with metallic junctions in which corrosion metallic wear debris is confirmed by histological/biomechanical examination. ALTR/ARMD such as osteolysis can also be associated with implant wear debris from other materials used for bearing surfaces in arthroplasty.

Three major features of ALTR/ARMD were identified as in need of a re-evaluation of the descriptive terminology used with a discussion of its implications for clinical evaluation, prognosis, and follow-up of the affected patients: pseudotumor, metallosis, and cell death and periprosthetic soft tissue/bone necrosis.

Pseudotumor

The use of the term pseudotumor for periprosthetic soft tissue reaction in total joint replacement can be found at least since the late 1980s[38,39] and was re-introduced in 2008[23] as a generic term to describe the periprosthetic soft tissue masses of variable size and content as a distinctive feature of ALTR/ARMD associated with the second generation of MoM implants.

A pseudotumor can be descriptively defined at macroscopic examination of the collected specimen as follows: a mass of variable size formed by the reactive proliferation of the joint pseudocapsule and neo-synovial membrane ranging from flat to cobblestone or papillary/polypoid configuration, with or without a layer of tissue necrosis/infarction and containing a variable amount of synovial fluid (present only if submitted separately after aspiration). A secondary, extracapsular pseudotumor with variable wall thickness and amount of fluid can be present with bursal involvement, in the majority of cases trochanteric but also of the iliopsoas region, due to the dehiscence of the synovial fluid through the detachment of the pseudocapsule. The wall of a pseudotumor is usually composed of an inner layer of residual native synovium not excised at primary surgery and/or newly formed synovium (neo-synovium/pseudocapsule) and of an outer layer of pre-existing connective tissue (capsule) of variable thickness. The fluid component varies in colour (brownish/greenish/pale to charcoal grey) and density ranging from watery to creamy depending mainly on the type of wear particles generated and the amount of exfoliated necrotic cell debris with the possible addition of blood products secondary to haemorrhage/chronic bleeding. The neo-synovial proliferation can be non-homogeneous around the cavity and can be more florid in locations where the particles of implant wear debris are generated and/or accumulated.

The term pseudotumor has been mistakenly used as a synonym for the lymphocytic-dominated type of ALTR/ARMD reaction associated or not with a variable degree of soft tissue/bone necrosis originally described as ALVAL.[20] However, the biological behaviour of a pseudotumor is dependent on the cell composition of the inflammatory infiltrate which can significantly influence its shape, size, wall thickness, and amount of fluid content.

Pseudotumors develop as intracapsular and/or extracapsular (bursal) masses and can be separated into two major categories:

Type I (early onset ALTR/ARMD) is characterized by a brisk reactive fibrovascular proliferation of the pseudocapsular/neo-synovial wall with or without effusion, which, in addition to the macrophage infiltrate with metallic particulate debris, requires the presence of a florid interstitial/perivascular lymphocytic component with possible addition of eosinophils, mast cells, plasma cells, neutrophils, and perivascular lymphocytic germinal centres in various combinations, as described in several publications of histopathological analysis.[24–29,31,32] This type of ALTR/ARMD may eventually progress to an advanced/end-stage of ALTR/ARMD of the adverse reaction with soft tissue necrosis with or without skeletal muscle and tendon involvement.

Type II (late onset ALTR/ARMD), characterized by a slow reactive proliferation of the pseudocapsular/neo-synovial wall with or without effusion with presence of an almost exclusive infiltrate of particle-laden macrophages and fibrovascular stromal proliferation with minimal interstitial/perivascular lymphocytic component and absence or presence of a variable degree of macrophage infiltration of the bone marrow which can lead to clinically significant periprosthetic osteolysis with aseptic loosening of implant components.[29,32]

Examples of intracapsular and extracapsular Type I and Type II pseudotumors are provided in Fig. 1 to Fig. 4.

Intracapsular Type I pseudotumor is shown in Fig. 1. Macroscopic polypoid configuration is evident (Fig. 1a) with corresponding tissue section, 11 mm thick (Fig. 1b, upper-left corner), composed of superficial macrophage infiltrate with marked interstitial lymphocytic infiltrate (Fig. 1c) and macrophages containing metallic wear debris from another area (Fig. 1c, inset). The tissue section of similar thickness in the lower-right corner (Fig. 1b) shows a more advanced stage of the adverse reaction with a superficial zone of necrotic soft tissue and underlying band of macrophage/lymphocytic infiltrate (Fig. 1d).

Intracapsular Type II pseudotumor is shown in Fig. 2. Papillary configuration is evident at macroscopic examination (Fig. 2a) and in the tissue section, 10 mm thick, with pseudocyst formed by invagination of the neosynovium (Fig. 2b), shown in detail with abundant exfoliation of necrotic macrophages (Fig. 2c), also shown at higher magnification (Fig. 2d). Extensive bone marrow involvement by particle-laden macrophage infiltrate
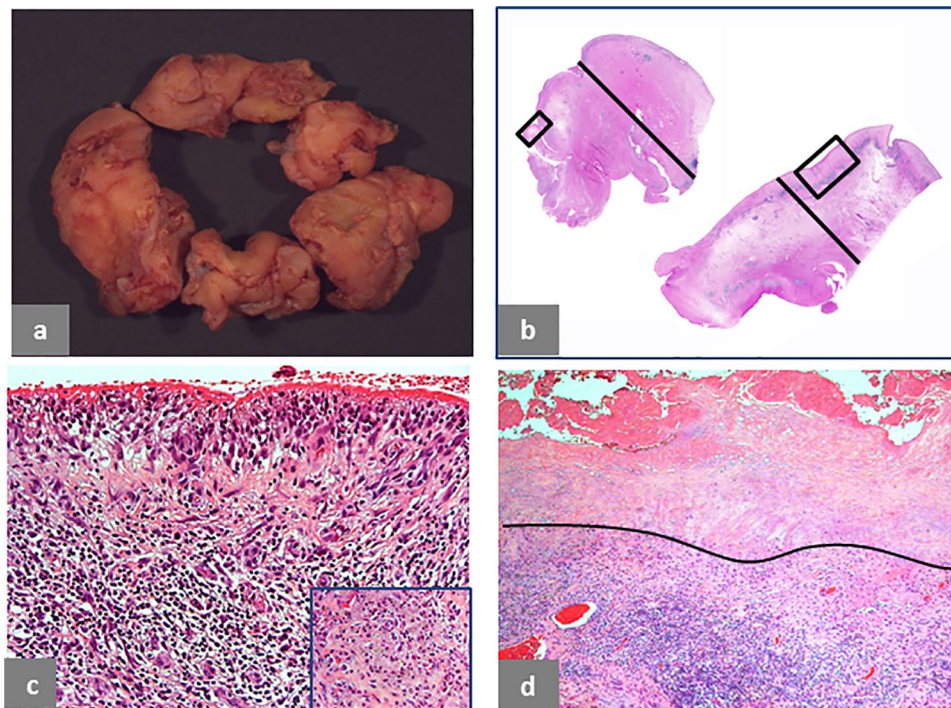
Fig. 1 Pseudotumor, solid, intracapsular. (a) Polypoid/papillary pattern of the neo-synovium, $6 \times 4 \times 1.2$ cm in greatest dimension. (b) Two histological sections from the neo-synovium showing polypoid hypertrophy with maximum thickness of 12 mm (black bar) of the upper tissue section and flat surface with maximum thickness of 10 mm (black bar) of the lower tissue section. (c) Detail of the area in the square box of the upper tissue section in b showing marked, interstitial lymphocytic infiltrate (H&E $\times$ 100). (d) Detail of the area in the square box of the lower tissue section in b showing superficial soft tissue necrosis above the black line and deep, predominantly lymphocytic inflammatory infiltrate (H&E $\times$ 50). The case is of a MoM LHTHA with CoCr MAS, implanted for 38 months, revised for hip pain with serum levels of Co 5.6 μg/L and Cr 4.2 μg/L. MRI demonstrated moderate wear-induced synovitis with low-intensity signal, consistent with metallic debris. There was fluid arising from the hip joint, which decompressed into the iliopsoas bursa, displacing the femoral nerve fascicles. There was no evidence of osteolysis.

Note. H&E, haematoxylin and eosin; MoM, metal-on-metal; LHTHA, large head total hip arthroplasty; Co, cobalt; Cr, chromium; MAS, metallic adapter sleeve; MRI, magnetic resonance imaging.

(Fig. 2e) is evident in the femoral head (inset) with disruption of the bone/implant interface surface proximally. The erosion of the bone interface by macrophage substitution is evident at higher magnification (Fig. 2f).

Extracapsular Type I pseudotumor is shown in Fig. 3. Cross-section of the open bursa shows necrotic papillary lining surface (Fig. 3a) with corresponding tissue section, 12 mm thick (Fig. 3 b). The wall shows full thickness tissue necrosis and deep-seated macrophage/lymphocytic inflammatory infiltrate (Fig. 3c), predominantly composed of lymphocytes and numerous eosinophils (Fig. 3d) with presence of a large aggregate of multi-layered corrosion products shown in inset.

Extracapsular Type II pseudotumor is shown in Fig. 4. The bursa shows a thin wall (Fig. 4a) with corresponding tissue section in the upper-left corner, 4 mm thick (Fig. 4b) and tissue section from the periprosthetic capsule of similar thickness in the lower-right corner (Fig. 4b). Details of the bursal wall show haemorrhagic, organized fibrinous exudate and macrophage infiltrate formation

of cholesterol crystals (Fig. 4c) and a large aggregate of green corrosion metallic particle from a different area shown in inset. The section of the periprosthetic neo-synovium shows more abundant haemorrhagic, organized fibrinous exudate and a fibrotic wall (Fig. 4d) with macrophage infiltrate containing metallic particles and hemosiderin deposits shown in inset.

In both cases of extracapsular pseudotumors, the histological features of the bursal neo-synovium where similar to those observed in the intracapsular soft tissue.

Bursal expansions (bursitis) are considered ALTR/ARMD clinically only if a connection between the joint capsule and the bursa is identified in the radiological studies. At histological examination, the presence of particle-laden macrophages and/or the presence of large aggregates of metallic particulate debris confirm the origin of the reaction from the joint fluid through the disruption of the capsular attachments.

The assumption that the mere presence of a mass defined as pseudotumor at radiological examination is
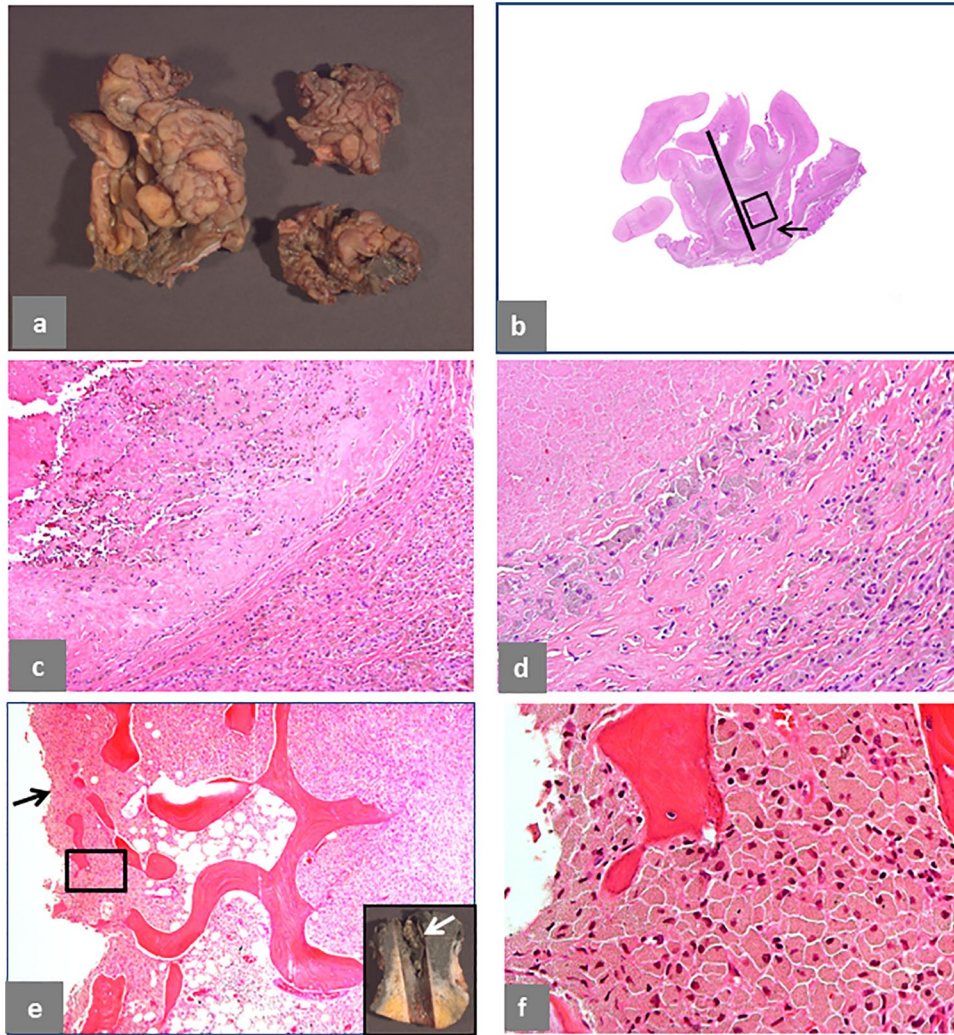
Fig. 2 Pseudotumor, solid with pseudocysts, intracapsular. (a) Papillary and polypoid pattern of the neo-synovium, 6 × 5 × 1 cm in greatest dimension. (b) Histological sections from the pseudocapsule with maximum thickness of 11 mm (black bar) and large pseudocyst (black arrow). (c) Detail of the area in the black box in b showing marked macrophage infiltrate with large amount of exfoliation of necrotic forms (H&E × 100). (d) Higher magnification of the macrophage infiltrate (H&E × 50). (e) Macrophage infiltrate in the femoral head cancellous bone with disruption of the interface membrane indicated by a black arrow (H&E × 200) as shown in the macroscopic image of the femoral head (white arrow). (f) Higher magnification of the macrophage infiltrate in the black box area in e showing high content of particulate metallic debris in the soft tissue with numerous needle-shaped particles (H&E × 400). The case is of a MoM HRA, implanted for 60 months, revised for serum levels of Co 27.2 μg/L and Cr 21.2 μg/L. MRI showed minimal non-specific synovial expansion, without evidence of severe adverse local tissue reaction to metallic wear debris.

Note. H&E, haematoxylin and eosin; MoM, metal-on-metal; HRA, hip resurfacing arthroplasty; Co, cobalt; Cr, chromium; MRI, magnetic resonance imaging.

diagnostic of the lymphocytic-dominated type of ALTR/ARMD is misleading because Type I and Type II pseudotumors can present with similar size and morphological features as shown in Figs. 1 to 4, and its definition cannot include a reliable threshold value for volume and wall thickness for the distinction of the two types. The amount of fluid content can be a significant component of its size which can vary during the implantation time; however, it is not as relevant as the cell composition of the infiltrate for the biological behaviour of the lesion. Prevalence of

pseudotumors/ALTR/ARMD has been found to be high in MoM HRA and MoM LHTHA implants even in asymptomatic patients and well-functioning implants in several reports[40–43] and also in MoM SHTHA[44,45] without detectable change in size or progression to soft tissue/skeletal muscle necrosis and/or neurovascular impingement. The main reason is because they are of Type II category and that progression/transformation from a macrophage reaction to a predominant lymphocytic type is usually not part of its clinicopathological course.[29] The predominant
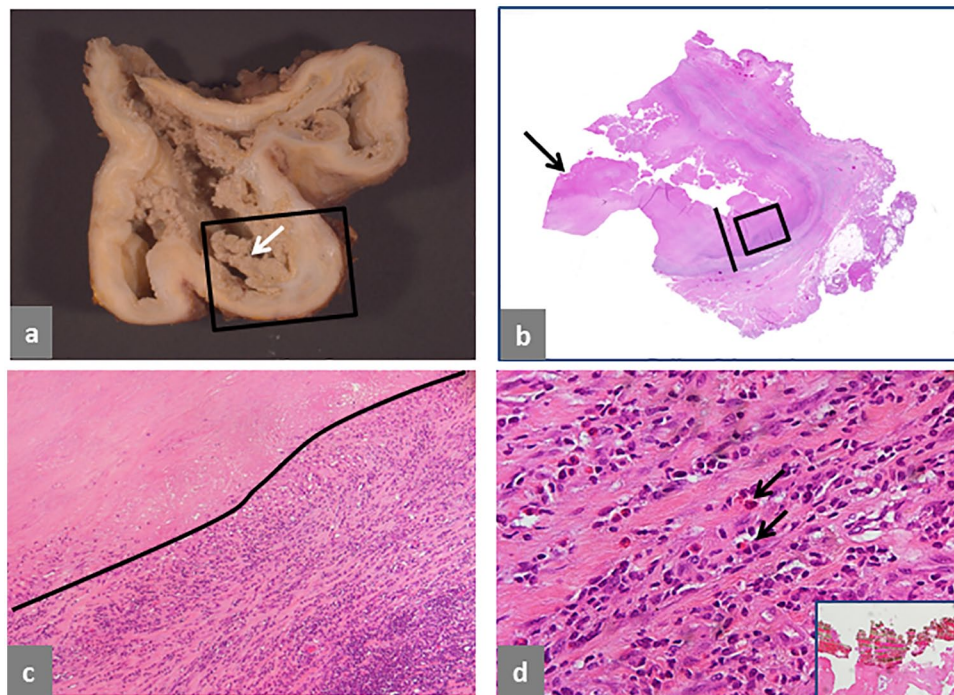
Fig. 3 Pseudotumor, mixed solid and cystic, extracapsular. (a) Trochanteric bursa, 12 × 10 × 8 cm with necrotic wall and papillary, necrotic neo-synovium (white arrow). (b) Histological section of the area in the black box in a showing wall thickness of 12 mm (black bar) and necrotic papilla (black arrow). (c) Detail of the bursal wall in the black box in b shows tissue necrosis and a large band of predominant lymphocytic infiltrate (H&E × 40). (d) Detail of the inflammatory infiltrate shows presence of numerous eosinophils indicated by black arrows (H&E × 400) and a large aggregate of greenish microplates of metallic corrosion particle aggregates alternating with red layers of blood products in inset (H&E × 200). The case is of a non-MoM THA with CoCr DMN and TMZF stem, implanted for 68 months, with pain in the gluteal area 13 months before revision and pseudotumor identified on MRI study after onset of symptoms. Serum levels of Co and Cr were not performed.

Note. H&E, haematoxylin and eosin; MoM, metal-on-metal; THA, total hip arthroplasty; CoCr, cobalt-chromium; DMN, dual modular neck; TMZF, Ti, Mo, Zr, Fe; MRI, magnetic resonance imaging.

medium- or long-term risk of ALTR/ARMD in this group is represented by the onset of bone marrow involvement by macrophage infiltrate with eventual osteolysis/implant loosening.[30] A comparison of the incidence of fluid collections or pseudotumors between MoM HRA and CoP THA has also been investigated using MRI[46] or CT,[47] showing a high prevalence also in non-MoM bearing surfaces. Histopathological and/or biomechanical analysis would be valuable to evaluate the possible clinical/biological importance of this finding, either for implant revision or for longitudinal follow-up.

The implications of the histopathological classification of pseudotumors in intracapsular and extracapsular Type I and Type II for correlation with the radiological studies (MRI, CT and ultrasound) are discussed in detail in Appendix I (see Supplementary Material link at the end of the article).

In summary, it is proposed that the term pseudotumor cannot be used as synonymous with ALTR/ARMD and not as a distinct category for any analysis of ALTR/ARMD. We have shown that Type I and Type II pseudotumors, either intracapsular or extracapsular, can be identified only by histopathological examination because the classification depends on the cellular composition of the inflammatory infiltrate and that Type II does not usually evolve in Type I during its clinicopathological course.

Metallosis

The term metallosis has been used at least since the early 1960s[48] without too much scrutiny regarding its clinical and biological significance. It has been applied in general to accumulation of metallic wear debris in periprosthetic tissue of large and small joints and also metallic fixation devices.[49–54] In arthroplasty, it has usually been described in case reports of a large amount of metallic wear debris in the synovial fluid/periprosthetic soft tissue secondary to catastrophic failure of implant components with toxic effects in various organs and systems generated by an extremely high blood concentration of metallic ions and in particular cobalt.[55] It has been used to describe metal debris usually from conventional wear due to friction by abrasion/adhesion/erosion, third-body wear, and also from
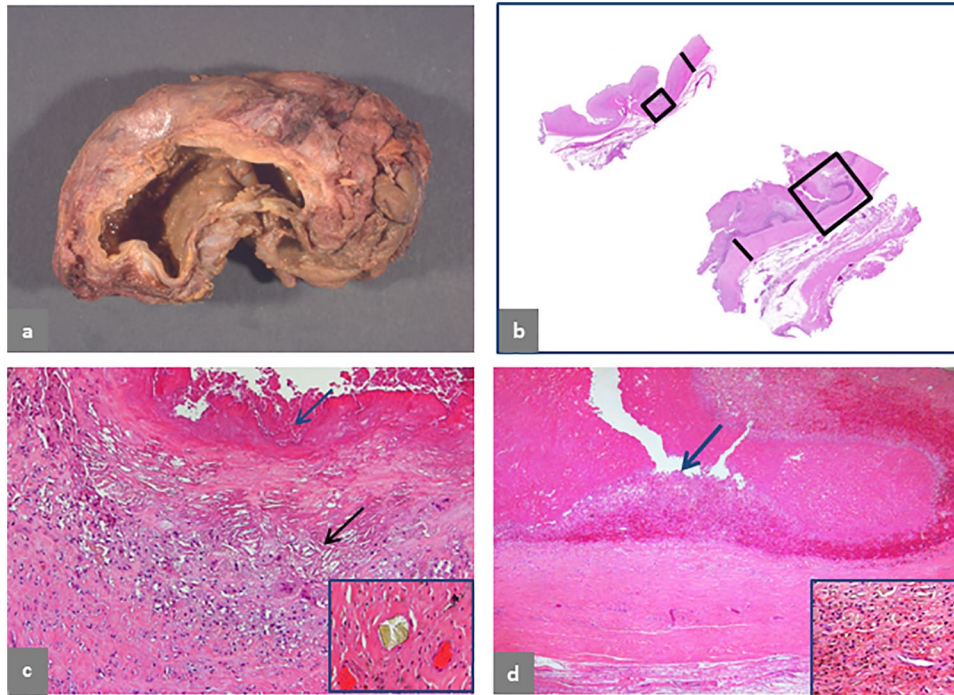
Fig. 4 Pseudotumor, predominantly cystic, extracapsular. (a) Trochanteric bursa, $9 \times 7 \times 5$ cm. (b) Wall of the bursa is shown in the upper section with 4 mm thickness (black bar) and wall of pseudocapsule is shown in the lower section with 4 mm thickness (black bar). (c) Detail of the area of the bursal wall in the small black box in b shows macrophage infiltrate with giant cells and formation of cholesterol crystal clefts (black arrow) and surface haemorrhagic exudate admixed with necrotic cell debris indicated by a blue arrow (H&E × 100) and a large, greenish microplate of corrosion metallic particles in inset (H&E × 200). (d) Detail of the area of the pseudocapsule in the large black box in b shows a similar configuration without presence of lymphocytic infiltrate and a thicker surface layer of haemorrhage and necrotic cell debris, indicated by a blue arrow (H&E × 50) with macrophage infiltrate containing metallic particles and haemosiderin deposits in inset (H&E × 400). The case is of a MoM LHTHA without MAS, implanted for 106 months, with symptoms of fullness in the gluteal area three months before revision and extracapsular pseudotumor identified on CT scan performed for unrelated abdominal pain. Serum levels of Co and Cr were not performed.

Note. H&E, haematoxylin and eosin; MoM, metal-on-metal; LHTHA, large head total hip arthroplasty; MAS, metallic adapter sleeve; CT, computerized tomography; Co, cobalt; Cr, chromium.

movement of loosened components in failing prostheses. These modes generate unintended wear debris resulting in increased local and systemic concentrations of metallic ions, predominantly chromium and cobalt with presence of a lesser amount of titanium and molybdenum.[56] On radiographs it has been described as a 'cloud', 'bubble', and 'metal-line' sign, all consisting in various shapes of increased radiodensity in the periprosthetic soft tissue,[56–59] on CT as soft tissue masses with radiointense walls[60] and on MRI studies as intra- and extracapsular soft tissue and bone marrow deposits of hypointense regions in proton-density weighted acquisitions.[61,62] At surgery, metallosis is defined by the macroscopic appearance of periprosthetic tissue and/or synovial fluid of greyish to jet-black colour.[63]

At histopathological examination, metallosis cannot be considered a diagnostic entity because it is defined only by the presence of a variable amount of conventional/corrosion metallic wear debris in the joint fluid, periprosthetic soft tissue and/or bone marrow without any measurable threshold as for the particulate wear debris of all other materials used in arthroplasty. A reliable measurement can be obtained only through quantification of total metal content per gram of dry tissue, although a range of values should be expected because of possible tissue selection and sample preparation/selection bias.[64,65] The definition of metallosis has more recently been expanded for the second generation of MoM HRA and THA implants with the addition of general terms such as taperosis, metallosis after hip resurfacing, modular neck metallosis[66] and later also trunnionosis for non-MoM implants with cobalt-chromium (CoCr) head and titanium (Ti) stem, without making a clear distinction between conventional and corrosion metallic wear and therefore adding uncertainty to its clinical significance. In addition, metallic debris can also be generated by fixation devices, such as broken metallic screws, indistinguishable from metallic wear debris both radiologically and histologically.
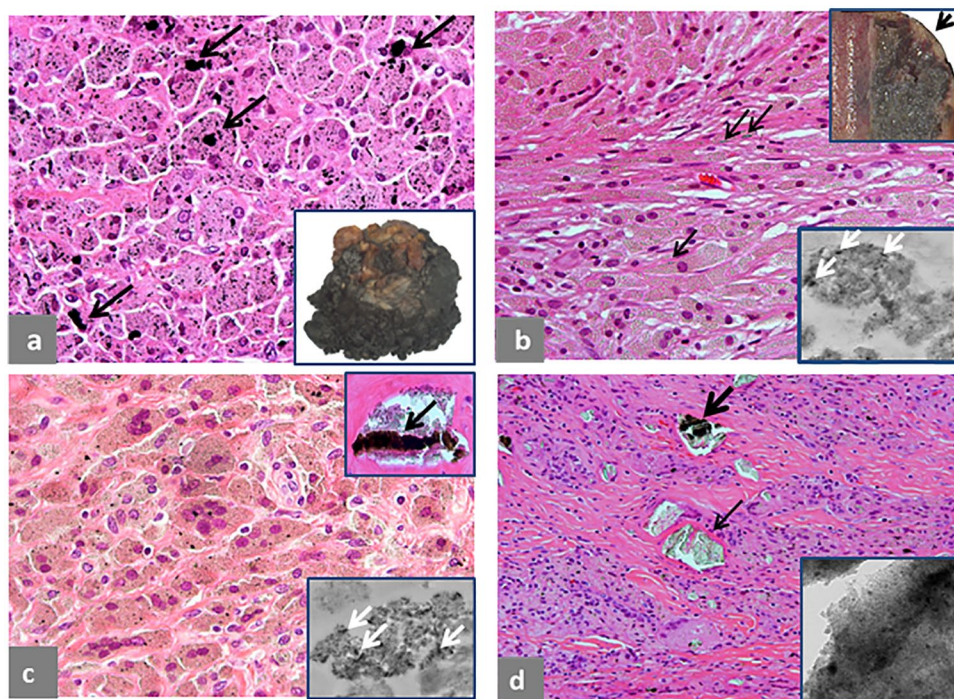
Fig. 5 Metallosis. (a) Macrophage infiltrate containing predominantly micro-particulate and occasionally macro-particulate (black arrows) conventional metallic debris in a case of MoP THA after 312 months of implantation with impingement of femoral neck/acetabular cup (H&E × 200) with formation of papillary, charcoal grey neo-synovium in inset. (b) Macrophage infiltrate in the bone marrow containing predominantly greenish/black, globular tribocorrosion aggregates/agglomerates of metallic nanoparticles and greenish/black needle-shaped metallic particles (black arrows), in a case of MoM HRA revised after 49 months of implantation with serum level of Co 71 μg/L and Cr 70 μg/L (H&E × 200); the bone surface is charcoal grey and partially lined by a cement cap indicated by a black arrow (upper-right inset) and the particle infiltrate showing electron-dense needle-shaped particles (white arrows) were rich in Co by TEM/SEM analysis (lower-right inset × 25000). (c) Macrophage infiltrate containing greenish/brownish tribocorrosion metallic particles and black metallic particles by mechanically assisted fretting/crevice corrosion, in a case of MoM LHTHA with CoCr MAS revised after 132 months of implantation with serum level of Co 84 μg/L and Cr 44 μg/L (H&E × 200); non-oxidized Ti-rich fragment is indicated by a black arrow (upper-right inset, H&E × 200) and larger, electron-dense particles (white arrows) were composed of CoCrTi by TEM/SEM analysis (lower-right inset × 20000). (d) Macrophage infiltrate containing scattered, irregular particles of greenish metallic particles by mechanically assisted fretting/crevice corrosion in a case of non-MoM THA with CoCr DMN and TMZF stem revised after 35 months of implantation with serum level of Co 7μg/L and Cr 5 μg/L and interstitial deposits of green microplates (thin black arrow) and green/black microplates (thick black arrow), shown to be aggregates/agglomerates of nanoparticles of co-localized metals (Co, Cr, Mo, Ti, Fe) by TEM/SEM analysis (inset × 50000).

Note. MoP, metal-on-polyethylene; THA, total hip arthroplasty; H&E, haematoxylin and eosin; MoM, metal-on-metal; HRA, hip resurfacing arthroplasty; Co, cobalt; Cr, chromium; TEM/SEM, transmission electron microscopy/scanning electron microscopy; LHTHA, large head total hip arthroplasty; MAS, metallic adapter sleeve; Ti, titanium; DMN, dual modular neck; TMZF, Ti, Mo, Zr, Fe; Mo, molybdenum; Fe, Iron.

Four cases diagnosed as metallosis at MRI examination and/or at surgery for different hip implants configurations are shown in Fig. 5. A case of MoP THA is shown Fig. 5a, with macrophage infiltrate containing predominantly micro-particulate and occasionally macro-particulate conventional metallic debris with formation of papillary, charcoal grey neo-synovium shown in inset. A case of MoM HRA is shown in Fig. 5b with macrophage infiltrate involving bone (osteolysis) with presence of tribocorrosion and conventional metallic particles by edge loading which confer a charcoal grey colour to the bone marrow of the femoral head (upper-right inset) and appear homogeneously greenish at microscopic examination secondary to oxidation during decalcification and haematoxylin and eosin

(H&E) staining, although clearly distinct by different electron density at TEM examination (lower-right inset). A case of MoM LHTHA with CoCr MAS is shown in Fig. 5c with large wear particle aggregate with black titanium component generated at the adapter sleeve/femoral neck taper junction in the upper-right inset, with different particle size, shape and electron density confirmed by TEM analysis in the lower-right inset. A case of non-MoM THA with CoCr DMN and TMZF stem is shown in Fig. 5d. In this instance, the neo-synovium does not show greyish/black colour and the corrosion metallic wear is generated only at the dual neck/stem interface with formation of large greenish aggregates of metallic nanoparticles in the periprosthetic soft tissue, confirmed by TEM/SEM analysis shown in inset.

The presented cases illustrate the complexity of the morphological and chemical features of the metallic wear debris and its ramifications in the understanding of the associated biological reactions. The consideration of metallosis in the MoM hip configuration as a distinctive diagnostic category is puzzling, since no other type of wear debris is possible and therefore all cases should be considered affected by a variable degree of metallosis. Moreover, the greyish-black colour of the synovial fluid and soft tissue used at surgery as the clinical/surgical criterion for the diagnosis applies only to conventional metallic particles rich in Co, Ti, and Zr generated by abrasion/adhesion/erosion, whereas Cr and Cr orthophosphate metallic particles generated by tribocorrosion or mechanically assisted crevice/fretting corrosion are oxidized in the synovial fluid and within the macrophages appear yellowish/greenish both at macroscopic examination and at light microscopy.[13] Although at histological examination particles generated by abrasion and impingement (Fig. 5a), tribocorrosion and edge loading (Fig. 5b), and predominantly mechanically assisted crevice/fretting corrosion (Fig. 5c, d) can share similarities of size and shape, at TEM/SEM analysis the particles generated at the modular junctions by corrosion modes are usually aggregates/agglomerates of nanoparticles mixed with organic material/fluid proteins forming complex particulate material of any size and shape (Fig. 5c, d). The formation of these aggregates was underestimated and not considered of major concern for host biological reactions at the time of implant design, approval process by regulatory authorities, marketing, and post-marketing short-term surveillance.

Since either conventional or corrosion metallic wear can be present in the same tissue in variable proportions during implantation time ranging from nanometres to microns and composed of a single metal or multiple metals in various combinations,[67–69] the chemistry of metallic particles from implant wear with the use of an analytical technique such as the recently described multiscale two-dimensional X-ray absorption spectroscopy (XAS) mapping can represent an additional, important contribution to the understanding of the biological reactions.[70] Accumulation of metallic particulate debris can also occur as an end point after multiple implant revisions with different materials, as shown in a case report with elemental analysis in which substantial in vivo exposure to particulate and dissociated tantalum, zirconium, chromium, cobalt, molybdenum, titanium, aluminium and vanadium was found with deposits in the periprosthetic soft tissue.[71] These results suggest that the in vivo occurrence of metallic wear debris can be more complex than predicted. In addition, any other modality of assessment of this type of wear, either by conventional histology[13] and/or using MRI-based techniques[72] could fall short of any predictive value for ALTR/ARMD especially in case of a high prevalence of Type II pseudotumor, limited to macrophage and fibroblastic reaction without lymphocytic infiltrate and/or soft tissue necrosis. As a consequence, the term metallosis, having originated as a relatively rare occurrence in arthroplasty of a large amount of metallic wear debris generated by abrasion/adhesion/fatigue, does not reflect the complexity of the conventional and corrosion metallic wear debris generated at the bearing surface and metallic modular junctions.

The issue of a dual role of metallic particles and ions is important in the occurrence and progression of the ALTR/ARMD reaction in the periprosthetic soft tissue and bone and it is discussed in Appendix II (see Supplementary Material link at the end of the article).

In summary, it is proposed that the term metallosis is not used as a category of implant failure or as a specific histological diagnosis and is substituted by presence of metallic wear debris with specification of conventional/corrosion/mixed when possible, as for all the other implant materials (polyethylene, ceramic, oxidized metal alloys, polymethyl methacrylate with radiographic contrast agent). The presence of fixation devices should also be reported in the pathology report, since they can be a possible origin of non-wear-related conventional and corrosion metallic debris. Additional studies are also needed to identify the effects on human macrophages and lymphocytes of corrosion metallic particles in vivo.

Cell death and periprosthetic soft tissue/bone necrosis

Two major types of necrosis can be observed in the cases of ALTR/ARMD: (a) cell death, predominantly of macrophages; (b) periprosthetic (neo-synovial/pseudocapsular/bone) tissue necrosis, defined as necrosis of cells and stromal elements (connective tissue, vessels, nerves). The correct identification of the two types of necrosis is important because, while cell necrosis occurs to a variable degree in all reactions to conventional and corrosion metallic wear debris and also other wear materials (polyethylene, ceramic), transmural soft tissue and/or bone necrosis is limited to a sub-group of patients with a predominantly lymphocytic response to corrosion metallic particles.[29,32]

Morphological features of cell necrosis are presented in Fig. 6. Macrophage necrosis can occur in the periprosthetic/bursal neo-synovium with formation of large clusters of foamy/xanthomatous forms exfoliating into the joint/bursal cavity (Fig. 6a) admixed to particle-laden macrophages shown in inset. The exfoliation of viable and necrotic macrophages into the joint space is shown in a toluidine blue stained semithin section (Fig. 6b) and corresponding H&E section shown in inset. The macrophage population exfoliated from the neo-synovial membrane (Fig. 6c) can form a thick slime as the one lodged in the groove of a large metallic femoral head (upper-right inset) with entrapped microplate aggregates of corrosion
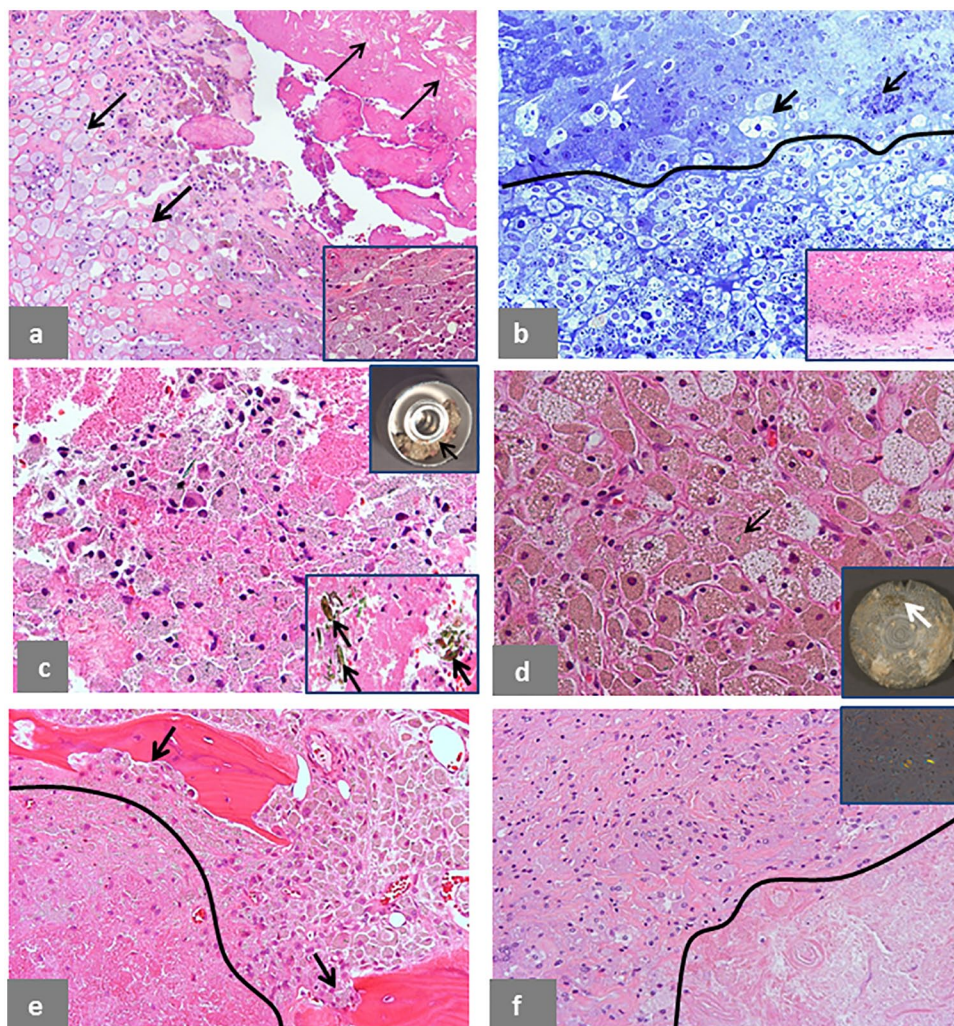
Fig. 6 Cell necrosis in ALTR/ARMD. (a) Macrophage necrosis in a bursal specimen (9 × 7 × 5 cm with wall thickness of 8 mm) in a case of MoM LHTHA with CoCr MAS revised after 100 months of implantation: macrophages at various stages of degeneration are indicated by the presence of many foamy forms (thick black arrows) with exfoliation of necrotic cell debris in the lumen with identifiable cholesterol crystal clefts indicated by thin black arrows (H&E × 100); details of the viable macrophages containing tribocorrosion metallic debris are shown in inset (H&E × 400). (b) Exfoliation of viable (white arrow) and necrotic macrophages (black arrows) from the neo-synovial surface is evident in a semithin section with separation of the surface from the necrotic cell debris by a black line (toluidine blue × 400) in a case of MoM HRA revised after 63 months of implantation with similar area stained by H&E shown in inset (H&E × 200). (c) A mixture of viable macrophages and necrotic cell debris in a case of MoM LHTHA with CoCr MAS with entrapped green particle aggregate of metallic debris (black arrow) collected from the debris present in the groove of the femoral head in the upper-right inset indicated by a black arrow (H&E × 200); large particle aggregates/agglomerates of corrosion products generated at the MAS/neck taper junction are shown in the lower-right inset, indicated by black arrows (H&E × 200). (d) A similar mixture of particle-laden macrophages with foamy forms is shown in tissue retrieved from the surface of the metallic acetabular shell (inset, white arrow) in a case of MoM LHTHA with CoCr MAS revised after 128 months of implantation also containing fragments of the larger green particle aggregates of metallic debris indicated by a black arrow (H&E × 400).
(e) Bone involvement by macrophage infiltrate with osteoclastic activity (black arrows) in a case of MoM HRA revised after 34 months of implantation with a large area of necrosis/infarct separated by a black line (H&E × 200). (f) A similar area of macrophage/infarct separated by a black line is shown in a case of MoP THA revised after 120 months of implantation (H&E × 200) with PE particles identifiable under polarized light in inset (H&E × 400).

Note. ALTR/ARMD, adverse local tissue reaction/adverse reaction to metal debris; MoM, metal-on-metal; LHTHA, large head total hip arthroplasty; CoCr, cobalt-chromium; MAS, metallic adapter sleeve; H&E, haematoxylin and eosin; HRA, hip resurfacing arthroplasty; MoP, metal-on-polyethylene; THA, total hip arthroplasty; PE, polyethylene.

metallic products (lower-right inset). A similar population of macrophages containing irregular, greenish aggregates of corrosion metallic particles can also be present in the bone marrow (Fig. 6d), forming a film on the acetabular cup shown in inset. Areas of cell necrosis most probably secondary to insufficient vascularization can also occur in the bone marrow of cases with osteolysis (Fig. 6e), although non-specific to MoM implants, as shown in the periprosthetic soft tissue of a case of polyethylene wear (Fig. 6f), shown under compensated polarized light in inset.

Cell death occurs through different modes: apoptosis by extrinsic and intrinsic pathways, autophagy, necrosis (oncosis), necroptosis, pyroptosis, and mitotic catastrophe.[73] It is not possible to determine the modality of cell death by histological examination at light microscopy and examination by TEM is necessary to examine fine morphological ultrastructural features. Moreover, a combination of morphological and biochemical classification of cell death is necessary for a more accurate diagnosis and similar cell deaths can have a high degree of functional and immunological differences.[73] The modality of cell death is important because it can affect the release of damage-associated molecular patterns (DAMPS) which can be immunogenic and initiate and perpetuate a non-infectious inflammatory response and can be triggered by many stimuli.[74] For macrophages, death occurs at a variable rate as a result of cytotoxicity of metallic ions/particles resulting in oxidative stress through the conversion of hydrogen peroxide into reactive hydroxyl radicals, direct binding to proteins inducing oxidation and loss of biological function, and displacement of other metal ions present in tissue metalloproteins affecting their activity.[33] Macrophage death occurs in MoM HRA implants secondary to formation of metallic wear by tribocorrosion (intended wear) and by edge loading (unintended wear) and in MoM LHTHA with or without CoCr MAS and also in non-MoM implants predominantly due to mechanically assisted fretting/crevice corrosion occurring at the metallic head/neck and/or neck/stem junctions. Corrosion has also been identified at the Ti acetabular cup/CoCr metallic liner interface,[75] although this is of undetermined biological significance. The valence of the metallic ions released by the implants is also considered a determinant of the degree of cellular toxicity, in particular the interaction of Cr (VI) with the macrophages.[76] Exfoliation of necrotic forms in the joint space is usually more pronounced in MoM LHTHA than in MoM HRA, probably secondary to the additional toxicity of the metallic wear generated at the head/neck junction. Recently, a mechanism of cell death with metallic wear debris mediated by electrochemical control via reduction-induced intrinsic apoptosis and oxidation-induced necrosis on CoCrMo alloy particles has been proposed and shown in vitro.[77]

The qualitative and quantitative analysis of macrophage necrosis is not confined to a mere scientific interest because the exfoliation of a large number of necrotic but also viable macrophages with release of secondary metallic particles is a continuous, dynamic process which can substantially affect the properties of the synovial fluid lubricating the bearing surface of the implant during its lifetime, and which cannot be easily reproduced by hip simulators or taken into account or measured by the examination of retrieved implants. Biotribology of artificial hip joints is complex[78] and the various degrees of cellular response to wear debris can modify the lubrication regime, affecting the fluid chemistry, thickness, and viscosity. Until now, this variable has not been considered in the formulation of the conventional lubrication models (boundary, elastohydrodynamic, and protein-aggregation) for MoM implants, and the synovial fluid analysis has been adjusted only for protein content, such as hyaluronan (HA), albumin and globulin without consideration either for the amount and composition of cell debris or the large particle aggregates of metallic wear debris generated at the head/neck junction of MoM LHTHA and neck/stem junction of non-MoM THA with CoCr DMN.[79] Although the degree of macrophage necrosis can vary depending on quantitative and qualitative aspects of the wear debris and host factors, its amount will increase during implantation time and remains a significant factor to be included in any study on the tribology of MoM and non-MoM hip arthroplasty. The presence of viable macrophages and multi-nucleated giant cells exfoliated into the synovial fluid provides support to the cellular mechanism of direct erosion of the metallic surface of the implant,[80–82] although some of the damage has been attributed to the use of electrocautery.[83,84]

Tissue necrosis is presented in Fig. 7. It can occur after an early proliferative phase of the neo-synovium with an accumulation of particle-laden macrophages and subsequent transmural infarction/necrosis of the soft tissue wall including newly formed papillary projections and the pre-existent capsule (Fig. 7a and 7b) with end-stage formation of a thick layer of transmural tissue necrosis (Fig. 7c and Fig. 7d) which occurred bilaterally in a case of non-MoM THA with CoCr DMN and TMZF stem previously diagnosed through ultrasound-guided needle biopsies (Fig. 7c, upper histological sections) and confirmed in the soft tissue specimen collected at implant revision time (Fig. 7c, lower histological section and Fig. 7d).

Full-thickness necrosis of neo-synovium and pseudocapsule has been generally considered coagulative and has been described only recently, representing the progression/end-stage of the lymphocytic-predominant ALTR/ARMD. It is almost invariably associated with a grade 3/4 perivascular and or/interstitial lymphocytic infiltrate if the interface of the pseudocapsule/adipose tissue is
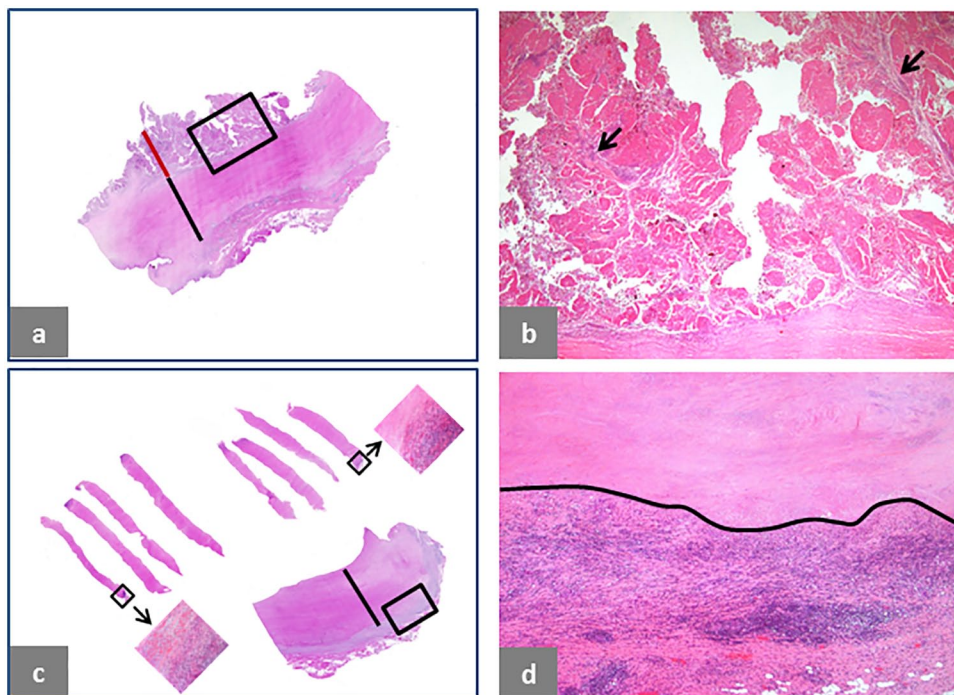
Fig. 7 Soft tissue necrosis in ALTR/ARMD. (a) Transmural necrosis of pre-existing pseudocapsule and papillary neo-synovium in a case of non-MoM CoCr DMN THA after 46 months of implantation with neo-synovium thickness of 8 mm (red bar) and pseudocapsule thickness of 12 mm (black bar) with underlying predominantly lymphocytic inflammatory infiltrate. (b) High power of the area shown in the black box in (a) showing complete necrosis of the neo-synovium with still identifiable stromal cores of the papillae indicated by black arrows (H&E × 25). (c) Transmural soft tissue necrosis with deep-seated inflammatory infiltrate in a case of non-MoM THA with CoCr DMN and TMZF stem after 24 months of implantation diagnosed bilaterally on ultrasound-guided fine-needle biopsy as shown in the upper sections (black boxes with arrows) and confirmed at revision surgery with thickness of the necrotic layer up to 9 mm (black bar). (d) Detail of the area in the black box of the lower tissue section in c shows upper zone of tissue necrosis/infarction separated by a black line from the deep-seated inflammatory infiltrate which is predominantly lymphocytic (H&E × 50).

Note. ALTR/ARMD, adverse local tissue reaction/adverse reaction to metal debris; MoM, metal-on-metal; CoCr, cobalt-chromium; DMN, dual modular neck; THA, total hip arthroplasty; H&E, haematoxylin and eosin; TMZF, Ti, Mo, Zr, Fe.

excised at surgery with a cold blade, although not all cases progress to this stage even after many years of implantation. The same histological pattern is observed in MoM and non-MoM implants and it is also invariably associated with corrosion metallic debris. A similar histological reaction has also been described in total knee arthroplasty (TKA) implants with corrosion metallic wear generated at the modular stem interface.[85–87] Hypoxia-inducible factor (HIF 1-α) pathway has been proposed to explain cobalt nanoparticle-induced cytotoxicity[88] and inflammation and also as a mechanism for metal-specific implant failure.[88,89] This hypothesis can explain mechanisms of macrophage necrosis, although it is not convincing as the trigger of the massive tissue necrosis of neo-synovium and pre-existing pseudocapsule observed in a subset of cases of ALTR/ARMD, and with particularly high prevalence in the non-MoM THA model with CoCr DMN and TMZF stem.[90,91] Because of the association between tissue necrosis, lymphocytic infiltrate, and corrosion metallic

debris, lymphocyte cytotoxicity and cell death should also be considered as a probable cause. For this reason, the contribution of different lymphocyte subsets to the pathogenic process should be studied in detail in relation to wear debris/protein corona complex and macrophage infiltrate.

Standard histological examination provides reliable and reproducible information regarding the presence of inflammatory cells, the rate of macrophage/soft tissue necrosis, and the type of particle aggregates generated by the implant bearing surface and junctions released into the synovial fluid. It can also provide a correlation and explanation for the variation of the fluid signal of the pseudo-tumors on T1- and T2-weighted images in ALTR/ARMD from hypointense to hyperintense representing a different content from water-like to proteinaceous or solid. In general, the necrotic cell debris and the particle content will increase during implantation time contributing to a denser fluid, although the total volume can be low especially if

Table 1. Grading of periprosthetic soft tissue and bone marrow lymphocytic infiltrate

Diffuse interstitial/band like lymphocytic infiltrate (CD45+ cells/mm^2)
0+ < 10
1+ 10 to 25
2+ 26 to 50
3+ 51 to 100
4+ > 100
Perivascular lymphoplasmacytic cuff/bone marrow lymphocytic aggregates*
0+ None to occasional
1+ < 0.25 mm
2+ 0.25 to 0.50 mm
3+ 0.51 to 0.75 mm
4+ > 0.75 mm
Number of lymphoplasmacytic perivascular aggregates
For grade 1: ≥ 5 aggregates; < 5 aggregates, non-specific
For cases of mixed grade: ≥ 3 aggregates of the highest grade present

*The presence of more than one germinal centre is classified as grade 4 with size of the aggregates > 0.25 mm.

Note. The clinical history of any treated or non-treated immunological disorder which can affect the size and composition of the lymphoplasmacytic infiltrates should be reported.

a predominant lymphocytic component with eosinophils and/or increased number of mast cells is not present.

In summary, it is proposed that macrophage cell necrosis should be distinguished from the transmural tissue necrosis observed in ALTR/ARMD and that they most probably occur through different pathways leading to distinct sub-types of necrosis. More research should be performed in this area elucidating the contribution to the final outcome of different cell populations, in particular macrophages, fibroblasts and lymphocytes.

ALTR/ARMD classifications

The classifications of ALTR/ARMD and their terminology are reviewed as well as the grading of the lymphocytic and macrophage infiltrate in periprosthetic soft tissue and bone. Since these classifications have been extensively used for clinical and radiological studies, it is important to discuss their categories and morphological features in detail, as presented in Appendix III (Tables 1 to 4 and Figs. 1 to 6) and Appendix IV (see Supplementary Material link at the end of the article).

In summary, the review of the available literature and the histological observations of the host reactions to metallic wear debris in the periprosthetic soft tissue and bone has provided the following results:

(a) Proposed classification of lymphocytic infiltrate through measurement of the infiltrate thickness over the row count and the requirement of a similar classification of lymphocytic infiltrate in the bone marrow (Table 1).

(b) Limited value of the macrophage semi-quantitative classification besides assessment of soft tissue and bone involvement and importance of evaluation

of the macrophage infiltrate in bone for osteolysis and interaction with haematopoietic cells.

(c) Undetermined role of mesenchymal stem cells, fibroblasts and endothelial cells in the onset and progression of ALTR/ARMD.

(d) Semi-quantitative assessment of lymphocytic infiltrate by H&E staining needs more analytical techniques (immunohistochemistry, immuno-fluorescence, flow cytometry) for a refined sub-classification of lymphocytes and other types of inflammatory cells.

(e) Need for a more comprehensive classification of delayed type hypersensitivity (DTH) reactions inclusive of its sub-types.

(f) Limited value of the histopathological classifications of periprosthetic soft tissue and bone for prognostic purposes and evaluation of long-term effects.

(g) Substitution of the acronym ALVAL and retention of ALTR and ARMD modified with the addition of the predominant cell type (lymphocytic or macrophage) as ALLTR/ALMRD and AMLTR/AMRMD.

An important aspect of the ALTR/ARMD classification is the definition of which type of reaction can be considered 'adverse', mainly for clinical but also for patients' compensation purposes. The adjective 'adverse' has a negative implication of some sort of damage which can be of short-, medium-, or long-term for the patient and also of different intensity and biological significance, as for all other immunologically mediated reactions. Although there is a general consensus to consider the predominantly lymphocytic reaction with periprosthetic soft tissue/bone necrosis in MoM and non-MoM implants as an adverse reaction to metallic wear debris, the definition and clinical significance of the macrophage reaction to metallic wear debris in MoM implants is more unclear, even in a setting of a pseudotumor.

The ALTR/ARMD generated by macrophages in the absence or minimal presence of a lymphocytic infiltrate is primarily represented by their bone invasion with the occurrence of osteolysis and eventual implant loosening requiring revision. Until the present time, non-septic osteolysis has been considered an unavoidable complication which has been addressed by modifications of the material composition and processing which affect the wear and the associated reaction, in for example the use of ultra-high molecular weight polyethylene (UHMWPE) with increased cross-linking and addition of antioxidant agents.[92] As a consequence, macrophage-induced osteolysis is not generally considered an adverse reaction specific to metallic wear debris and is included in the broad category of implant aseptic loosening by national implant registries and regulatory authorities. This current assessment might be in need of a re-evaluation. In the case of MoM implants

if the degree of macrophage death were considered to exceed the natural death rate, the consequent changes in the lubrication film would lead to increased wear from the bearing surface and modular junctions, significantly affecting the lifetime of the implant, and the increase in the motility of the macrophages would produce a spike in cases of clinically significant macrophage-induced osteolysis even after a long implantation time.

In summary, from a medical and biological point of view it would be unwise to attempt to predict or exclude local and/or systemic long-term complications based on a relatively short time of observation and therefore the significance of the term 'adverse' in these immune reactions remains an open question which can be answered with some degree of confidence only through a lifetime longitudinal follow-up of large cohorts of patients.

Natural history of ALTR/ARMD

The natural history (pathological progression) of ALTR/ARMD can vary significantly according to implant configuration, amount and type of particle wear, and host reaction. However, recurrent patterns of ALTR/ARMD can be accurately described through the observation of many cases of the same implant configuration of a single or multiple manufacturers and extensive tissue sampling at surgery and macroscopic examination. Histological examination of the intact bursal specimens can provide important clues regarding the early phase of ALTR/ARMD, because the bursa is involved at later implantation time than the capsular neo-synovium by dehiscence of the synovial fluid containing wear particles through the capsule and represents a closed system of variable volume and thickness. Examples of the natural history of ALTR/ARMD are provided in Fig. 8 and Fig. 9.

The progression from proliferative to necrotic tissue phase in a case of predominant lymphocytic reaction with macrophage component in a case of non-MoM THA with CoCr DMN and TMZF stem is shown in Fig. 8a–e: the wall is composed of a florid papillary neo-synovial proliferation (red bar) and the pre-existing capsule (black bar) in the upper section from the posterior pseudocapsule (Fig. 8a) with surface cellular proliferation composed of macrophages and giant cells (Fig. 8b), shown at higher magnification with scattered particle aggregates of corrosion metallic wear debris (Fig. 8c) and detail of a giant cell containing a corrosion particle aggregate shown in inset. A more advanced stage of the reaction is shown in the lower section from the inferior pseudocapsule (Fig. 8a) with formation of a thick layer of transmural soft tissue necrosis with coalescence and/or partial loss of the papillary component, shown in detail (Fig. 8d) with higher magnification of the lymphocytic infiltrate shown in inset. In a limited number of cases, the extension of the lymphocytic infiltrate into the adjacent skeletal muscle with subsequent fibre necrosis can also occur (Fig. 8e). The development of a predominant macrophage reaction to tribocorrosion in a case of MoM HRA is shown in Fig. 8f–h. The neo-synovium has papillary configuration (Fig. 8f) with macrophage infiltrate without lymphocytic component (Fig. 8g) shown at higher magnification in inset and in the massive macrophage infiltrate in the bone marrow (Fig. 8h), causing osteolysis of the femoral head shown in inset with loosening of the cup. A case of macrophage reaction with bursal component of a MoM LHTHA implant is shown in Fig. 9a–d: the large bursa in Fig. 9a with internal lining surface shown in inset; in Fig. 9b, the upper sections show the bursal neo-synovium compared to the lower section of the neo-synovium of the pseudocapsule; micropapillary hypertrophy of the bursal neo-synovium is evident without perivascular lymphocytic infiltrate (Fig. 9c) with detail of the macrophage infiltrate (Fig. 9d) also observed in the pseudocapsule.

The correlation with the variation in the radiological findings of the ALTR/ARMD is provided in Appendix V (see Supplementary Material link at the end of the article). In particular, the chronological evolution of the reactions is discussed, and its correlation with the three parameters used for MRI classification of their severity: fluid component, wall thickness/cystic component, solid component and the dependence of the parameters on the type of wear generated by the implant and the host response (qualitative and quantitative cell composition of the inflammatory infiltrate).

In summary, it is shown that the assessment of the natural history of ALTR/ARMD requires the knowledge of at least its cell composition which can be provided before implant revision only by the histopathological examination of the periprosthetic tissue through biopsies (ultrasound-guided fine core needle or arthroscopic forceps) and that the study of its evolution requires a large number of observations because of the cross-sectional nature of the histopathological examination.

Risk of prosthetic joint infection in MoM implants

Although prosthetic joint infection (PJI) is considered a complication of joint arthroplasty and not a form of ALTR/ARMD, its classification might change if a higher prevalence is found in MoM and non-MoM hip implants at risk for ALTR/ARMD. In a retrospective study of 104 cases of failed MoM HRA and THA hip arthroplasty, a relatively higher prevalence of PJI was found (6.7%) compared to other bearing surface combinations, with similar bacterial species.[93] The findings have been supported by other studies on acute delayed infection in failed MoM THA[94] and in a comparative study of MoM THA versus other hip bearing surfaces on a large population.[95] Therefore, monitoring of this cohort of patients could be prudent with
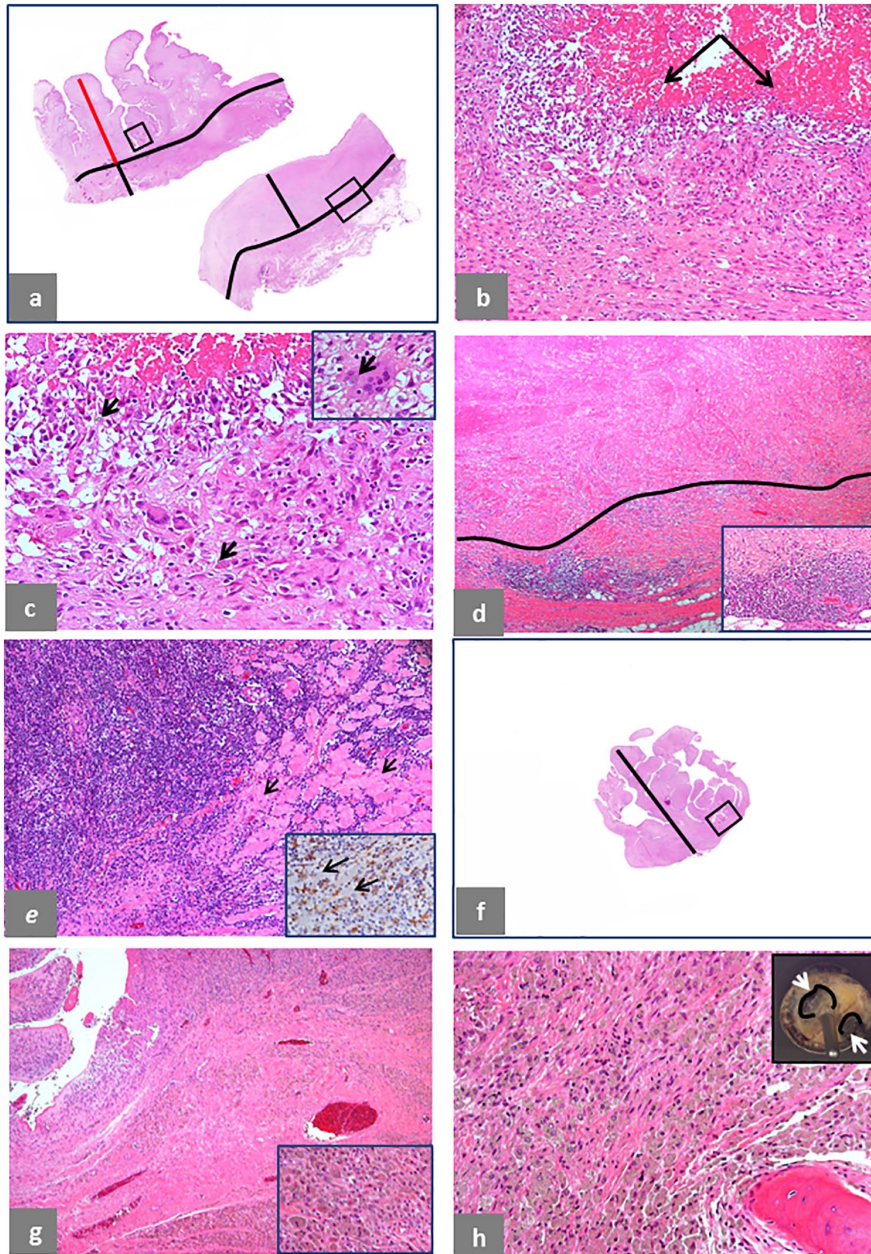
Fig. 8 Pseudotumor natural history, intracapsular. (a) Case of predominantly lymphocytic ALTR/ARMD in a non-MoM THA with CoCr DMN and TMZF stem revised after 20 months of implantation: area of florid papillary neo-synovium (upper section), 13 mm thick (red bar) and underlying pseudocapsule, 5 mm thick (black bar) with a black line separating the two zones; area of transmural necrosis (lower section), 12 mm thick (black bar), separated from the zone of viable fibroadipose tissue by a black line. (b) The area in the black box of the upper tissue section in (a) shows florid macrophage infiltrate with numerous giant cells and marked exfoliation of necrotic forms indicated by black arrows (H&E × 100). (c) Higher magnification shows scattered particles of corrosion metallic debris indicated by black arrows (H&E × 200) and engulfed in a giant cell indicated by a black arrow in inset (H&E × 400). (d) The area in the black box of the lower tissue section in (a) shows a necrotic zone separated by a black line from the underlying viable vascular layer with marked lymphocytic infiltrate at the interface (H&E × 40) with higher magnification in inset (H&E × 200). (e) Extension of the lymphocytic infiltrate to the underlying skeletal muscle fibres (black arrows) with a 'polymyositis pattern' (H&E × 100) and predominant T-cell CD8+ component around muscle fibres (black arrows) shown in inset (× 400). (f) Case of macrophage ALTR/ARMD in a MoM HRA revised after 79 months of implantation and serum level of Co 6.6 μg/L and Cr 20.4 μg/L: section of papillary hypertrophy, 15 mm thick (black bar). (g) The area in the black box of the tissue section in (f) shows florid macrophage infiltrate (H&E × 100) with higher magnification in inset (H&E × 400). (h) Bone invasion by florid, particle-laden macrophage infiltrate (H&E × 100) in the femoral head with two areas of osteolysis (white arrows) circled by a black line in inset.

Note. ALTR/ARMD, adverse local tissue reaction/adverse reaction to metal debris; MoM, metal-on-metal; THA, total hip arthroplasty; CoCr, cobalt-chromium; DMN, dual modular neck; TMZF, Ti, Mo, Zr, Fe; H&E, haematoxylin and eosin; HRA, hip resurfacing arthroplasty.
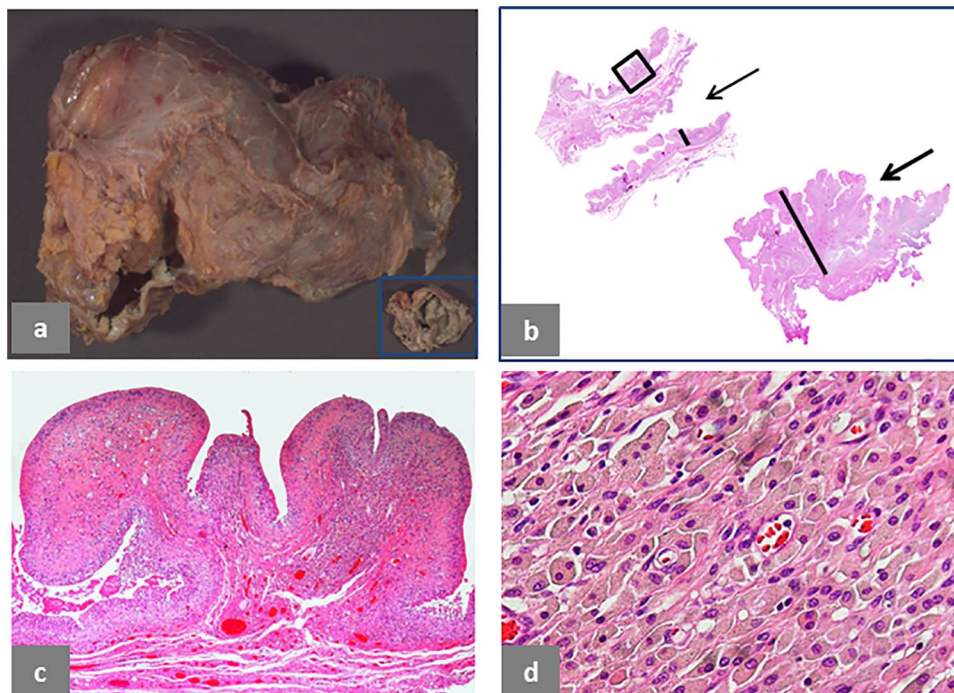
Fig. 9 Pseudotumor natural history, extracapsular. (a) Trochanteric bursa 8 × 5 × 4 cm in a case of MoM LHTHA with CoCr MAS revised after 94 months of implantation (Co 3 μg/L; Cr 7.5 μg/L) with internal surface of the bursa shown in inset. (b) Two sections of the bursal wall (upper-left corner) with maximum thickness of 4 mm (black bar) and section of the intracapsular neo-synovium (lower-right corner) with maximum thickness of 15 mm (black bar). (c) Papillary configuration of the bursal synovium of the area in the square box in a (H&E × 40). (d) Macrophage infiltrate containing greenish, predominantly globular aggregates of tribocorrosion metallic particles (H&E × 400).

Note. H&E, haematoxylin and eosin; MoM, metal-on-metal; LHTHA, large head total hip arthroplasty; CoCr, cobalt-chromium; MAS, metallic adapter sleeve; H&E, haematoxylin and eosin.

investigation on the risk factors involved in the local environment induced by metallic corrosion products and ions generated by the implants.

Histopathological examination and post-marketing surveillance

For post-marketing surveillance, the histopathological examination of the periprosthetic tissue through ultrasound-guided or arthroscopic biopsy and/or at revision surgery of failed joint implants can provide two major contributions: (1) The identification of 'sentinel' cases of early onset ALTR/ARMD (preferably with correlated biomechanical analysis of the implant) to be submitted to regulatory authorities and national implant registries for immediate monitoring of the implants at risk, before their possible identification in the registries' annual reports; (2) The use of the histopathological classification of ALTR/ARMD for the evaluation of the occurrence of its sub-types during longitudinal follow-up.

The identification of the histological type of ALTR/ARMD is important and a major indicator for the implementation of a successful risk stratification algorithm for the clinical management of patients implanted with MoM HRA and THA devices. In the USA, the use of MoM bearing surfaces declined from 40.1 % in 2008 to 9.8% in 2012 and 4% in 2014.[96] Similar trends have been observed in the Australian Orthopaedic Association National Joint Replacement Registry and the National Joint Registry for England, Wales, Northern Ireland and the Isle of Man. Therefore, it is reasonable to assume that the great majority of the second-generation MoM LHTHA cohorts are currently at least six years post-arthroplasty with a large number of them approaching 10 years or longer time of implantation. Although a similar decline has been experienced for the MoM HRA, this configuration is still being implanted in selected centres worldwide, especially the Birmingham hip resurfacing (BHR) model.

If the macrophage type of ALTR/ARMD without or with minimal lymphocytic infiltrate were the most frequent at medium- and long-term implant life as suggested,[29] recent studies based on data including the cohort with predominant lymphocytic reaction would not reflect the current trend of ALTR/ARMD and would be of limited value for the longitudinal follow-up at the present time and in the future. In this setting, the use of blood levels of

Co, Cr and also Ti as an effective and relatively inexpensive method for monitoring MoM HRA and MoM THA at medium- and long-term implant life,[97,98] and especially of metal ion trends,[99] is supported by the histopathological analysis of the revised cases. The upward trend of Co and Cr values at sequential measurements with a time interval of one or two years would be considered an index of risk for impending implant failure, because of excessive wear and/or micro-motion of implant components leading eventually to macrophage-induced osteolysis and loosening. It should be assessed using radiological exams, such as metal artifact reduction sequences (MARS) MRI and MAR CT scans, taking into account that the femoral head of MoM HRA cannot be visualized underneath the metal cup for the presence of osteolysis.

Several studies have been conducted with the aim of identifying serum Co and Cr threshold values between well-functioning and poorly-functioning implants[100,101] or for the identification of patients at risk of ARMD.[102–104] The latter have been more controversial than the former with a commentary of praise[105] as well as criticism.[106] The majority of the objections are linked to the terminology used for the analysis and they are addressed in this publication which could lead to a re-evaluation of the conclusions reached in these studies. It is important to notice that in one study,[98] the serum level of Co and Cr >20 µg/L has been proposed as the threshold value for considering implant revision because of the possibility of systemic toxicity. In the cases shown in Fig. 5b and Appendix III (see Supplementary Material link at the end of the article) Fig. 5a and 5f, the values of Co and Cr at the time of revision were much higher than this threshold value, raising the doubt that the standards provided by scientific studies are consistently applied in the clinical practice. The case illustrated in Appendix III Fig. 5d shows that early osteolysis can occur at Co and Cr levels lower than 20 µ/L, further indicating the need for longitudinal follow-up also for MoM HRA patients.

It is important to emphasize that the histopathological examination of the periprosthetic tissue cannot be used to predict the risk of long-term local effects and short- and long-term systemic effects, especially because of the complexity of the conventional and corrosion metallic debris and metallo-organic compounds and their possible migration to lymph nodes, bone marrow, and distant organs.[107] The examination of metal toxicity is beyond the scope of this article; however, although cases of metal toxicity secondary to orthopaedic implants have been found to be infrequently reported in the scientific literature,[108] it would be reasonable to follow the prudent approach which has been advocated with development of a management plan for Co and Cr levels in the range of 10 µg/L and of a validated symptom scoring system for all patients.[109] At last, it needs to be taken into proper consideration that brain-specific changes of structure and function have been reported associated with chronic metal exposure to Co blood levels of 1.72 µg/L and Cr blood levels of 1.42 µg/L,[110] indicating that there might not be any safe threshold for chronic exposure to metallic debris.

In summary, the assumption that all MoM implants would perform well after some years of relatively stable levels of serum Co and Cr without the need for any further monitoring could be misleading at best or disastrous at worst for an unknown number of implanted patients, especially because the macrophage type of reaction is predominantly asymptomatic, possibly giving a false sense of security to patients and providers as well.

Conclusions

Several terms of major use in the description of ALTR and ARMD and the parameters for its classification have been examined and changes of clinical significance in the terminology used have been proposed. The comparison between the histopathological diagnosis of ALTR and ARMD and the classifications used for radiological diagnosis regarding their natural history has provided insights useful for all disciplines involved in their diagnosis, management, and long-term surveillance. However, the use of a common terminology and of a unified and validated classification for ALTR and ARMD is only a necessary step forward and does not guarantee a better understanding of the complex mechanisms which contribute to their onset and progression.

Periprosthetic tissue sampling for histopathological analysis should become a standard procedure at revision surgery. A free consultation service online could be implemented by national implant registries with the participation of an international panel of expert pathologists. Identification of implants at risk, more precise criteria for implant revision, and elucidation of the mechanisms of particle wear–host interaction can happen only through a close cooperation between clinical and basic research disciplines.

The histopathological analysis can provide critical data for the improvement of current methods and models of research and the development of a new strategy for pre-marketing testing and post-marketing surveillance. The limitations of the histopathological examination for predicting the risk of medium- and long-term effects of ALTR and ARMD, either local or systemic have also been examined in depth.

Efforts should also be made by the scientific community to engage with a critical eye in translational multi-disciplinary research with the utilization of real-world data through the use of in silico systems of analysis with the goal of identifying risk predictors and possible biomarkers for the assessment of orthopaedic implant performance as recently suggested.[111]

EFORT open reviews

AUTHOR INFORMATION

[1]Department of Orthopedics and Orthopedic Surgery, University Medicine Greifswald, Greifswald, Germany.

[2]Division of Orthopaedics and Traumatology, Fondazione Policlinico Universitario Agostino Gemelli IRCCS, Rome, Italy.

[3]Department of Pathology and Laboratory Medicine, Sinai Health System, Toronto, Canada.

[4]Centre for Nanohealth, Swansea University Medical School, Singleton Park, Swansea, UK.

[5]Department of Orthopaedics, Faculty of Medicine and Dentistry, University Hospital, Palacky University Olomouc, Czech Republic.

[6]Department of Pathology, University Hospital of North Tees and Hartlepool NHS Foundation Trust, Stockton-on-Tees, UK.

[7]Orthopaedic Department, Freeman Hospital, Newcastle upon Tyne, UK.

[8]Pathologisch-bakteriologisches Institut, Otto Wagner Spital, Wien, Austria.

[9]Servicio de Cirugía Ortopédica y Traumatología, Hospital Universitario La Paz-IdiPAZ, Universidad Autónoma de Madrid, Madrid, Spain.

[10]MVZ-Zentrum für Histologie, Zytologie und Molekulare Diagnostik-GmbH, Trier, Germany.

Correspondence should be sent to: Dr. Giorgio Perino, Klinik und Poliklinik für Orthopädie und Orthopädische Chirurgie Universitätsmedizin Greifswald Sauerbruchstrasse 17475 Greifswald Germany.
Email: giorgio.perino@med.uni-greifswald.de

ICMJE CONFLICT OF INTEREST STATEMENT

DL reports consultancy and expert testimony, acting as witness for plaintiff in metal-on-metal hip litigation for PXD Ltd trading as ExplantLab, and a filed patent to identify risk of ARMD using genetic algorithm with PXD Ltd, all outside the submitted work.
The other authors declare no conflict of interest relevant to this work.

SUPPLEMENTAL MATERIAL

Supplemental material is available for this paper at https://online.boneandjoint.org.uk/doi/suppl/10.1302/2058-5241.6.210013

REFERENCES

1. Learmonth ID, Young C, Rorabeck C. The operation of the century: total hip replacement. *Lancet* 2007;370:1508–1519.

2. Amstutz HC, Le Duff MJ. Hip resurfacing: history, current status, and future. *Hip Int* 2015;25:330–338.

3. Ranawat AS, Ranawat CS. The history of total knee arthroplasty. In: *The knee joint*. Paris: Springer-Verlag, 2012:699–707.

4. Johal S, Nakano N, Baxter M, Hujazi I, Pandit H, Khanduja V. Unicompartmental knee arthroplasty: the past, current controversies, and future perspectives. *J Knee Surg* 2018;31:992–998.

5. Flatow EL, Harrison AK. A history of reverse total shoulder arthroplasty. *Clin Orthop Relat Res* 2011;469:2432–2439.

6. Prkić A, van Bergen CJA, The B, Eygendaal D. Total elbow arthroplasty is moving forward: review on past, present and future. *World J Orthop* 2016;7:44–49.

7. McBeath R, Osterman AL. Total wrist arthroplasty. *Hand Clin* 2012;28:595–609.

8. Gougoulias NE, Khanna A, Maffulli N. History and evolution in total ankle arthroplasty. *Br Med Bull* 2009;89:111–151.

9. Adkinson JM, Chung KC. Advances in small joint arthroplasty of the hand. *Plast Reconstr Surg* 2014;134:1260–1268.

10. Mirra JM, Amstutz HC, Matos M, Gold R. The pathology of the joint tissues and its clinical relevance in prosthesis failure. *Clin Orthop Relat Res* 1976;117:221–240.

11. Willert HG, Semlitsch M. Reactions of the articular capsule to wear products of artificial joint prostheses. *J Biomed Mater Res* 1977;11:157–164.

12. Doorn PF, Mirra JM, Campbell PA, Amstutz HC. Tissue reaction to metal on metal total hip prostheses. *Clin Orthop Relat Res* 1996;329:S187–S205.

13. Perino G, Sunitsch S, Huber M, et al. Diagnostic guidelines for the histological particle algorithm in the periprosthetic neo-synovial tissue. *BMC Clin Pathol* 2018;18:7.

14. DiCarlo EF, Bullough PG. The biologic responses to orthopedic implants and their wear debris. *Clin Mater* 1992;9:235–260.

15. Gibon E, Amanatullah DF, Loi F, et al. The biological response to orthopaedic implants for joint replacement. Part I: metals. *J Biomed Mater Res B Appl Biomater* 2017;105:2162–2173.

16. Gibon E, Córdova LA, Lu L, et al. The biological response to orthopedic implants for joint replacement. II: Polyethylene, ceramics, PMMA, and the foreign body reaction. *J Biomed Mater Res B Appl Biomater* 2017;105:1685–1691.

17. Bauer TW, Schils J. The pathology of total joint arthroplasty. I. Mechanisms of implant fixation. *Skeletal Radiol* 1999;28:423–432.

18. Bauer TW, Schils J. The pathology of total joint arthroplasty. II. Mechanisms of implant failure. *Skeletal Radiol* 1999;28:483–497.

19. Krenn V, Morawietz L, Perino G, et al. Revised histopathological consensus classification of joint implant related pathology. *Pathol Res Pract* 2014;210:779–786.

20. Davies AP, Willert HG, Campbell PA, Learmonth ID, Case CP. An unusual lymphocytic perivascular infiltration in tissues around contemporary metal-on-metal joint replacements. *J Bone Joint Surg Am* 2005;87:18–27.

21. Schmalzried TP. Metal-metal bearing surfaces in hip arthroplasty. *Orthopedics* 2009;32:orthosupersite.com/view.asp?rID=42831.

22. Langton DJ, Jameson SS, Joyce TJ, Hallab NJ, Natu S, Nargol AV. Early failure of metal-on-metal bearings in hip resurfacing and large-diameter total hip replacement: a consequence of excess wear. *J Bone Joint Surg Br* 2010;92:38–46.

23. **Pandit H, Glyn-Jones S, McLardy-Smith P, et al.** Pseudotumours associated with metal-on-metal hip resurfacings. *J Bone Joint Surg Br* 2008;90:847–851.

24. **Mahendra G, Pandit H, Kliskey K, Murray D, Gill HS, Athanasou N.** Necrotic and inflammatory changes in metal-on-metal resurfacing hip arthroplasties. *Acta Orthop* 2009;80:653–659.

25. **Huber M, Reinisch G, Trettenhahn G, Zweymüller K, Lintner F.** Presence of corrosion products and hypersensitivity-associated reactions in periprosthetic tissue after aseptic loosening of total hip replacements with metal bearing surfaces. *Acta Biomater* 2009;5:172–180.

26. **Campbell P, Ebramzadeh E, Nelson S, Takamura K, De Smet K, Amstutz HC.** Histological features of pseudotumor-like tissues from metal-on-metal hips. *Clin Orthop Relat Res* 2010;468:2321–2327.

27. **Natu S, Sidaginamale RP, Gandhi J, Langton DJ, Nargol AV.** Adverse reactions to metal debris: histopathological features of periprosthetic soft tissue reactions seen in association with failed metal on metal hip arthroplasties. *J Clin Pathol* 2012;65:409–418.

28. **Grammatopoulos G, Pandit H, Kamali A, Maggiani F, Glyn-Jones S, Gill HS, et al.** The correlation of wear with histological features after failed hip resurfacing arthroplasty. *J Bone Joint Surg Am* 2013;95:e81 (1–10).

29. **Ricciardi BF, Nocon AA, Jerabek SA, et al.** Histopathological characterization of corrosion product associated adverse local tissue reaction in hip implants: a study of 285 cases. *BMC Clin Pathol* 2016;16:3.

30. **Gallo J, Vaculova J, Goodman SB, Konttinen YT, Thyssen JP.** Contributions of human tissue analysis to understanding the mechanisms of loosening and osteolysis in total hip replacement. *Acta Biomater* 2014;10:2354–2366.

31. **Mittal S, Revell M, Barone F, et al.** Lymphoid aggregates that resemble tertiary lymphoid organs define a specific pathological subset in metal-on-metal hip replacements. *PLoS One* 2013;8:e63470.

32. **Perino G, Ricciardi BF, Jerabek SA, et al.** Implant based differences in adverse local tissue reaction in failed total hip arthroplasties: a morphological and immunohistochemical study. *BMC Clin Pathol* 2014;14:39.

33. **Scharf B, Clement CC, Zolla V, et al.** Molecular analysis of chromium and cobalt-related toxicity. *Sci Rep* 2014;4:5729.

34. **Kolatat K, Perino G, Wilner G, et al.** Adverse local tissue reaction (ALTR) associated with corrosion products in metal-on-metal and dual modular neck total hip replacements is associated with upregulation of interferon gamma-mediated chemokine signaling. *J Orthop Res* 2015;33:1487–1497.

35. **Catelas I, Lehoux EA, Ning Z, Figeys D, Baskey SJ, Beaulé PE.** Differential proteomic analysis of synovial fluid from hip arthroplasty patients with a pseudotumor vs. periprosthetic osteolysis. *J Orthop Res* 2018;36:1849–1859.

36. **Krenn V, Perino G.** *Histological diagnosis of implant-associated pathologies.* Germany: Springer-Verlag Berlin Heidelberg, 2017.

37. **Bauer TW.** CORR insights: current pathologic scoring systems for metal-on-metal THA revisions are not reproducible. *Clin Orthop Relat Res* 2017;475:3012–3014.

38. **Griffiths HJ, Burke J, Bonfiglio TA.** Granulomatous pseudotumors in total joint replacement. *Skeletal Radiol* 1987;16:146–152.

39. **Svensson O, Mathiesen EB, Reinholt FP, Blomgren G.** Formation of a fulminant soft-tissue pseudotumor after uncemented hip arthroplasty: a case report. *J Bone Joint Surg Am* 1988;70:1238–1242.

40. **Hart AJ, Satchithananda K, Liddle AD, et al.** Pseudotumors in association with well-functioning metal-on-metal hip prostheses: a case-control study using three-dimensional computed tomography and magnetic resonance imaging. *J Bone Joint Surg Am* 2012;94:317–325.

41. **Fehring TK, Odum S, Sproul R, Weathersbee J.** High frequency of adverse local tissue reactions in asymptomatic patients with metal-on-metal THA. *Clin Orthop Relat Res* 2014;472:517–522.

42. **Bisschop R, Boomsma MF, Van Raay JJ, Tiebosch AT, Maas M, Gerritsma CL.** High prevalence of pseudotumors in patients with a Birmingham Hip Resurfacing prosthesis: a prospective cohort study of one hundred and twenty-nine patients. *J Bone Joint Surg Am* 2013;95:1554–1560.

43. **Hjorth MH, Mechlenburg I, Soballe K, Roemer L, Jakobsen SS, Stilling M.** Higher prevalence of mixed or solid pseudotumors in metal-on-polyethylene total hip arthroplasty compared with metal-on-metal total hip arthroplasty and resurfacing hip arthroplasty. *J Arthroplasty* 2018;33:2279–2286.

44. **Moon JK, Kim Y, Hwang KT, Yang JH, Ryu JA, Kim YH.** Prevalence and natural course of pseudotumours after small-head metal-on-metal total hip arthroplasty: a minimum 18-year follow-up study of a previous report. *Bone Joint J* 2019;101-B:317–324.

45. **D'Angelo F, Tanas D, Gallazzi E, Zagra L.** Adverse reaction to metal debris after small-head diameter metal-on-metal total hip arthroplasty: an increasing concern. *Hip Int* 2018;28:35–42.

46. **Bisseling P, de Wit BW, Hol AM, van Gorp MJ, van Kampen A, van Susante JL.** Similar incidence of periprosthetic fluid collections after ceramic-on-polyethylene total hip arthroplasties and metal-on-metal resurfacing arthroplasties: results of a screening metal artefact reduction sequence-MRI study. *Bone Joint J* 2015;97-B:1175–1182.

47. **van der Veen HC, Reininga IH, Zijlstra WP, Boomsma MF, Bulstra SK, van Raay JJ.** Pseudotumour incidence, cobalt levels and clinical outcome after large head metal-on-metal and conventional metal-on-polyethylene total hip arthroplasty: mid-term results of a randomised controlled trial. *Bone Joint J* 2015;97-B:1481–1487.

48. **Straumann F, Steinemann S, Pohler O, Willenegger H, Schenk R.** Recent experimental and clinical results in metallosis. *Langenbecks Arch Klin Chir Ver Dtsch Z Chir* 1963;305:21–28.

49. **Beaulé PE, Campbell P, Amstutz HC.** Metallosis and metal-on-metal bearings. *J Bone Joint Surg Am* 2000;82:751–752.

50. **Korovessis P, Petsinis G, Repanti M, Repantis T.** Metallosis after contemporary metal-on-metal total hip arthroplasty: five to nine-year follow-up. *J Bone Joint Surg Am* 2006;88:1183–1191.

51. **Milošev L, Antolič V, Minovič A, et al.** Extensive metallosis and necrosis in failed prostheses with cemented titanium-alloy stems and ceramic heads. *J Bone Joint Surg Br* 2000;82:352–357.

52. **Gogna P, Paladini P, Merolla G, Augusti CA, Maddalena F, Porcellini G.** Metallosis in shoulder arthroplasty: an integrative review of literature. *Musculoskelet Surg* 2016;100:3–11.

53. **Heyes GJ, Julian HS, Mawhinney I.** Metallosis and carpal tunnel syndrome following total wrist arthroplasty. *J Hand Surg Eur Vol* 2018;43:448–450.

54. **Teoh KH, von Ruhland C, Evans SL, et al.** Metallosis following implantation of magnetically controlled growing rods in the treatment of scoliosis: a case series. *Bone Joint J* 2016;98-B:1662–1667.

55. **Bradberry SM, Wilkinson JM, Ferner RE.** Systemic toxicity related to metal hip prostheses. *Clin Toxicol (Phila)* 2014;52:837–847.

56. Lombardi AV Jr, Mallory TH, Staab M, Herrington SM. Particulate debris presenting as radiographic dense masses following total knee arthroplasty. *J Arthroplasty* 1998;13:351–355.

57. Su EP, Callander PW, Salvati EA. The bubble sign: a new radiographic sign in total hip arthroplasty. *J Arthroplasty* 2003;18:110–112.

58. Paydar A, Chew FS, Manner PA. Severe periprosthetic metallosis and polyethylene liner failure complicating total hip replacement: the cloud sign. *Radiol Case Rep* 2015;2:115.

59. Weissman BN, Scott RD, Brick GW, Corson JM. Radiographic detection of metal-induced synovitis as a complication of arthroplasty of the knee. *J Bone Joint Surg Am* 1991;73:1002–1007.

60. Kirkham JR, Petscavage JM, Richardson ML. Metallosis: CT findings in a total hip arthroplasty. *Radiol Case Rep* 2015;5:410.

61. Nawabi DH, Gold S, Lyman S, Fields K, Padgett DE, Potter HG. MRI predicts ALVAL and tissue damage in metal-on-metal hip arthroplasty. *Clin Orthop Relat Res* 2014;472:471–481.

62. Koff MF, Esposito C, Shah P, et al. MRI of THA correlates with implant wear and tissue reactions: a cross-sectional study. *Clin Orthop Relat Res* 2019;477:159–174.

63. Cipriano CA, Issack PS, Beksaç B, Della Valle AG, Sculco TP, Salvati EA. Metallosis after metal-on-polyethylene total hip arthroplasty. *Am J Orthop (Belle Mead NJ)* 2008;37:E18–E25.

64. Buly RL, Huo MH, Salvati E, Brien W, Bansal M. Titanium wear debris in failed cemented total hip arthroplasty: an analysis of 71 cases. *J Arthroplasty* 1992;7:315–323.

65. Kuba M, Gallo J, Pluháček T, Hobza M, Milde D. Content of distinct metals in periprosthetic tissues and pseudosynovial joint fluid in patients with total joint arthroplasty. *J Biomed Mater Res B Appl Biomater* 2019;107:454–462.

66. Fehring KA, Fehring TK. Modes of failure in metal-on-metal total hip arthroplasty. *Orthop Clin North Am* 2015;46:185–192.

67. Xia Z, Ricciardi BF, Liu Z, et al. Nano-analyses of wear particles from metal-on-metal and non-metal-on-metal dual modular neck hip arthroplasty. *Nanomedicine (Lond)* 2017;13:1205–1217.

68. Di Laura A, Quinn PD, Panagiotopoulou VC, et al. The chemical form of metal species released from corroded taper junctions of hip implants: synchrotron analysis of patient tissue. *Sci Rep* 2017;7:10952.

69. Kovochich M, Fung ES, Donovan E, Unice KM, Paustenbach DJ, Finley BL. Characterization of wear debris from metal-on-metal hip implants during normal wear versus edge-loading conditions. *J Biomed Mater Res B Appl Biomater* 2018;106:986–996.

70. Morrell AP, Floyd H, Mosselmans JFW, et al. Improving our understanding of metal implant failures: multiscale chemical imaging of exogenous metals in ex-vivo biological tissues. *Acta Biomater* 2019;98:284–293.

71. Schoon J, Geißler S, Traeger J, et al. Multi-elemental nanoparticle exposure after tantalum component failure in hip arthroplasty: in-depth analysis of a single case. *Nanomedicine (Lond)* 2017;13:2415–2423.

72. Koch KM, Koff MF, Bauer TW, et al. Off-resonance based assessment of metallic wear debris near total hip arthroplasty. *Magn Reson Med* 2018;79:1628–1637.

73. Galluzzi L, Baehrecke EH, Ballabio A, et al. Molecular definitions of autophagy and related processes. *EMBO J* 2017;36:1811–1836.

74. Vanlangenakker N, Vanden Berghe T, Vandenabeele P. Many stimuli pull the necrotic trigger, an overview. *Cell Death Differ* 2012;19:75–86.

75. Hothi HS, Ilo K, Whittaker RK, Eskelinen A, Skinner JA, Hart AJ. Corrosion of metal modular cup liners. *J Arthroplasty* 2015;30:1652–1656.

76. Lalaouni A, Henderson C, Kupper C, Grant MH. The interaction of chromium (VI) with macrophages: depletion of glutathione and inhibition of glutathione reductase. *Toxicology* 2007;236:76–81.

77. Hui T, Kubacki GW, Gilbert JL. Voltage and wear debris from Ti-6Al-4V interact to affect cell viability during in-vitro fretting corrosion. *J Biomed Mater Res A* 2018;106:160–167.

78. Di Puccio F, Mattei L. Biotribology of artificial hip joints. *World J Orthop* 2015;6:77–94.

79. Myant C, Cann P. On the matter of synovial fluid lubrication: implications for metal-on-metal hip tribology. *J Mech Behav Biomed Mater* 2014;34:338–348.

80. Gilbert JL, Sivan S, Liu Y, Kocagöz SB, Arnholt CM, Kurtz SM. Direct in vivo inflammatory cell-induced corrosion of CoCrMo alloy orthopedic implant surfaces. *J Biomed Mater Res A* 2015;103:211–223.

81. DiLaura A, Hothi HS, Meswania JM, et al. Clinical relevance of corrosion patterns attributed to inflammatory cell-induced corrosion: a retrieval study. *J Biomed Mater Res B Appl Biomater* 2017;105:155–164.

82. Cerquiglini A, Henckel J, Hothi HS, Di Laura A, Skinner JA, Hart AJ. Inflammatory cell-induced corrosion in total knee arthroplasty: a retrieval study. *J Biomed Mater Res B Appl Biomater* 2018;106:460–467.

83. Kubacki GW, Sivan S, Gilbert JL. Electrosurgery induced damage to Ti-6Al-4V and CoCrMo alloy surfaces in orthopedic implants in vivo and in vitro. *J Arthroplasty* 2017;32:3533–3538.

84. Yuan N, Park SH, Luck JV Jr, Campbell PA. Revisiting the concept of inflammatory cell-induced corrosion. *J Biomed Mater Res B Appl Biomater* 2018;106:1148–1155.

85. Arnholt CM, MacDonald DW, Tohfafarosh M, et al; Implant Research Center Writing Committee. Mechanically assisted taper corrosion in modular TKA. *J Arthroplasty* 2014;29:205–208.

86. Arnholt CM, MacDonald DW, Malkani AL, et al; Implant Research Center Writing Committee. Kocagöz SB, Gilbert JL M. Corrosion damage and wear mechanisms in long-term retrieved CoCr femoral components for total knee arthroplasty. *J Arthroplasty* 2016;31:2900–2906.

87. Christiner T, Pabbruwe MB, Kop AM, Parry J, Clark G, Collopy D. Taper corrosion and adverse local tissue reactions in patients with a modular knee prosthesis. *JBJS Open Access* 2018;3:e0019.

88. Nyga A, Hart A, Tetley TD. Importance of the HIF pathway in cobalt nanoparticle-induced cytotoxicity and inflammation in human macrophages. *Nanotoxicology* 2015;9:905–917.

89. Samelko L, Caicedo MS, Lim S-J, Della-Valle C, Jacobs J, Hallab NJ. Cobalt-alloy implant debris induce HIF-1α hypoxia associated responses: a mechanism for metal-specific orthopedic implant failure. *PLoS One* 2013;8:e67127.

90. Meftah M, Haleem AM, Burn MB, Smith KM, Incavo SJ. Early corrosion-related failure of the rejuvenate modular total hip replacement. *J Bone Joint Surg Am* 2014;96:481–487.

91. Nawabi DH, Do HT, Ruel A, et al. Comprehensive analysis of a recalled modular total hip system and recommendations for management. *J Bone Joint Surg Am* 2016;98:40–47.

92. Bracco P, Bellare A, Bistolfi A, Affatato S. Ultra-high molecular weight polyethylene: influence of the chemical, physical, and mechanical properties on the wear behavior. A review. *Materials (Basel)* 2017;10:1–22.

93. Grammatopoulos G, Munemoto M, Inagaki Y, Tanaka Y, Athanasou NA. The diagnosis of infection in metal-on-metal hip arthroplasties. *J Arthroplasty* 2016;31: 2569—2573.

94. Prieto HA, Berbari EF, Sierra RJ. Acute delayed infection: increased risk in failed metal on metal total hip arthroplasty. *J Arthroplasty* 2014;29:1808—1812.

95. Kleeman LT, Bala A, Penrose CT, Seyler TM, Wellman SS, Bolognesi MP. Comparison of postoperative complications following metal-on-metal total hip arthroplasty with other hip bearings in medicare population. *J Arthroplasty* 2018;33: 1826—1832.

96. Heckmann ND, Sivasundaram L, Stefl MD, Kang HP, Basler ET, Lieberman JR. Total hip arthroplasty bearing surface trends in the United States from 2007 to 2014: the rise of ceramic on polyethylene. *J Arthroplasty* 2018;33:1757—1763.e1.

97. Sidaginamale RP, Joyce TJ, Lord JK, et al. Blood metal ion testing is an effective screening tool to identify poorly performing metal-on-metal bearing surfaces. *Bone Joint Res* 2013;2:84—95.

98. Connelly JW, Galea VP, Matuszak SJ, Madanat R, Muratoglu O, Malchau H. Indications for MARS-MRI in patients treated with metal-on-metal hip resurfacing arthroplasty. *J Arthroplasty* 2018;33:1919—1925.

99. Carlson BC, Bryan AJ, Carrillo-Villamizar NT, Sierra RJ. The utility of metal ion trends in predicting revision in metal-on-metal total hip arthroplasty. *J Arthroplasty* 2017;32:S214—S219.

100. Van Der Straeten C, Grammatopoulos G, Gill HS, Calistri A, Campbell P, De Smet KA. The 2012 Otto Aufranc Award: the interpretation of metal ion levels in unilateral and bilateral hip resurfacing. *Clin Orthop Relat Res* 2013;471:377—385.

101. Donahue GS, Galea VP, Laaksonen I, Connelly JW, Muratoglu O, Malchau H. Establishing thresholds for metal ion levels in patients with bilateral Articular Surface Replacement hip arthroplasty. *Hip Int* 2019;29:475—480.

102. Matharu GS, Berryman F, Brash L, Pynsent PB, Treacy RB, Dunlop DJ. The effectiveness of blood metal ions in identifying patients with unilateral Birmingham Hip Resurfacing and Corail-Pinnacle metal-on-metal hip implants at risk of adverse reactions to metal debris. *J Bone Joint Surg Am* 2016;98:617—626.

103. Matharu GS, Berryman F, Brash L, Pynsent PB, Dunlop DJ, Treacy RB. Can blood metal ion levels be used to identify patients with bilateral Birmingham Hip Resurfacings who are at risk of adverse reactions to metal debris? *Bone Joint J* 2016;98-B:1455—1462.

104. Matharu GS, Berryman F, Judge A, et al. Blood metal ion thresholds to identify patients with metal-on-metal hip implants at risk of adverse reactions to metal debris: an external multicenter validation study of Birmingham Hip Resurfacing and Corail-Pinnacle implants. *J Bone Joint Surg Am* 2017;99:1532—1539.

105. Dorr LD. Metal-on-metal testing to salvage a device disaster: commentary on an article by Gulraj S. Matharu, BSc(Hons), MBChB, MRCS, MRes, et al.: 'The effectiveness of blood metal ions in identifying patients with unilateral Birmingham Hip Resurfacing and Corail-Pinnacle metal-on-metal hip implants at risk of adverse reactions to metal debris'. *J Bone Joint Surg Am* 2016;98:e31.

106. Campbell P, Ebramzadeh E. ARMD and presumed dangerous! Commentary on an article by Gulraj S. Matharu, BSc(Hons), MRCS, MRes, et al.: 'Blood metal ion thresholds to identify patients with metal-on-metal hip implants at risk of adverse reactions to metal debris. An external multicenter validation study of Birmingham Hip Resurfacing and Corail-Pinnacle implants'. *J Bone Joint Surg Am* 2017;99:e100.

107. Hall DJ, Pourzal R, Jacobs JJ, Urban RM. Metal wear particles in hematopoietic marrow of the axial skeleton in patients with prior revision for mechanical failure of a hip or knee arthroplasty. *J Biomed Mater Res B Appl Biomater* 2019;107:1930—1936.

108. Zywiel MG, Cherian JJ, Banerjee S, et al. Systemic cobalt toxicity from total hip arthroplasties: review of a rare condition Part 2. measurement, risk factors, and step-wise approach to treatment. *Bone Joint J* 2016;98-B:14—20.

109. Gessner BD, Steck T, Woelber E, Tower SS. A systematic review of systemic cobaltism after wear or corrosion of chrome-cobalt hip implants. *J Patient Saf* 2019;15:97—104.

110. Clark MJ, Prentice JR, Hoggard N, Paley MN, Hadjivassiliou M, Wilkinson JM. Brain structure and function in patients after metal-on-metal hip resurfacing. *AJNR Am J Neuroradiol* 2014;35:1753—1758.

111. Dabic S, Azarbaijani Y, Karapetyan T, et al. Development of an integrated platform using multidisciplinary real-world data to facilitate biomarker discovery for medical products. *Clin Transl Sci* 2020;13:98—109.